Molecular Pharmacology Fast Forward. Published on October 25, 2012 as doi:10.1124/mol.112.081182
This article has not been copyedited and formatted. The final version may differ from this version.

Title Page:

N-arachidonyl glycine (NAGly) does not activate G protein-coupled receptor 18 (GPR18) signaling via canonical pathways

Van B. Lu, Henry L. Puhl III, and Stephen R. Ikeda

Section on Transmitter Signaling, Laboratory of Molecular Physiology, National Institute on Alcohol Abuse and Alcoholism, National Institutes of Health, Bethesda, Maryland, 20892-9411

Molecular Pharmacology Fast Forward. Published on October 25, 2012 as DOI: 10.1124/mol.112.081182
This article has not been copyedited and formatted. The final version may differ from this version.

Running Title Page:

Running title:

Lack of GPR18 activation by NAGly

Mailing address of corresponding author:

Stephen R. Ikeda, M.D., Ph.D.

Laboratory of Molecular Physiology

NIH/NIAAA

5625 Fishers Lane, Room TS-11, MSC 9411

Bethesda, MD, 20892, USA (regular mail)

Rockville, MD, 20852, USA (express mail)

Telephone: (301) 443-2807

Fax: (301) 480-8035

Email: sikeda@mail.nih.gov

Text: 61 pages

Tables: 2

Figures: 10 figures + 3 supplemental figures

References: 55

Abstract: 235 words

Introduction: 497 words

Discussion: 1399 words

Molecular Pharmacology Fast Forward. Published on October 25, 2012 as DOI: 10.1124/mol.112.081182
This article has not been copyedited and formatted. The final version may differ from this version.

Abbreviations list:

NAGly: N-arachidonyl glycine

GPR18: G protein-coupled receptor 18

GPCR: G protein-coupled receptors

AEA: anandamide, N-arachidonylethanolamide

Abn-Cbd: abnormal cannabidiol

MAPK: mitogen-activated protein kinase

DNA: deoxyribonucleic acid

PCR: polymerase chain reaction

EGFP: enhanced green fluorescent protein

HA: hemagglutinin

ADRA2A: α_{2A}-adrenergic receptor

MEM: minimum essential medium

PEI: polyethylenimine

DPBS: Dulbecco's phosphate buffered saline

BSA: bovine serum albumin

Qdot®655: quantum dot 655

RT: room temperature

TBS-T: Tris buffered saline with 0.05% Tween-20

NA: numerical aperature

PVDF: polyvinylidene difluoride

SCG: superior cervical ganglion

EBSS: Earles' balanced salt solution

Molecular Pharmacology Fast Forward. Published on October 25, 2012 as DOI: 10.1124/mol.112.081182
This article has not been copyedited and formatted. The final version may differ from this version.

TEA-OH: tetraethylammonium hydroxide

HEPES: 4-(2-hydroxyethyl)-1-piperazineethanesulfonic acid

EGTA: ethylene glycol tetraacetic acid

TTX: tetrodotoxin

PTX: pertussis toxin

CTX: cholera toxin

BRET: bioluminescence resonance energy tranfer

HEK: human embryonic kidney

CAMYEL: cAMP sensor using YFP-Epac-RLuc

cAMP: cyclic adenosine monophosphate

CNS: central nervous system

ANOVA: analysis of variance

FAAH: fatty acid amide hydrolase

Molecular Pharmacology Fast Forward. Published on October 25, 2012 as DOI: 10.1124/mol.112.081182
This article has not been copyedited and formatted. The final version may differ from this version.

Abstract:

Recent studies propose that N-arachidonyl glycine (NAGly), a carboxylic analog of anandamide, is an endogenous ligand of the $G\alpha_{i/o}$ protein-coupled receptor 18 (GPR18). However, a high-throughput β-arrestin-based screen failed to detect activation of GPR18 by NAGly (Yin et al., 2009; *JBC*, 18:12328). To address this inconsistency, we investigated GPR18 coupling in a native neuronal system with endogenous signaling pathways and effectors. We heterologously expressed GPR18 in rat sympathetic neurons and examined the modulation of N-type ($Ca_v2.2$) calcium channels. Proper expression and trafficking of receptor was confirmed by the "rim-like" fluorescence of fluorescently-tagged receptor and the positive staining of external hemagglutinin-tagged GPR18-expressing cells. Application of NAGly on GPR18-expressing neurons did not inhibit calcium currents, but instead potentiated currents in a voltage-dependent manner, similar to what has previously been reported (Guo et al., 2008; *J Neurophysiol*, 100:1147). Other proposed agonists of GPR18, including anandamide and abnormal cannabidiol, also failed to induce inhibition of calcium currents. Mutants of GPR18, designed to constitutively activate receptors, did not tonically inhibit calcium currents indicating a lack of GPR18 activation or coupling to endogenous G proteins. Other downstream effectors of $G\alpha_{i/o}$-coupled receptors, G protein-coupled inwardly-rectifying potassium channels and adenylate cyclase, were not modulated by GPR18 signaling. Furthermore, GPR18 did not couple to other G proteins tested: $G\alpha_s$, $G\alpha_z$ and $G\alpha_{15}$. These results suggest NAGly is not an agonist for GPR18 or that GPR18 signaling involves non-canonical pathways not examined in these studies.

Molecular Pharmacology Fast Forward. Published on October 25, 2012 as DOI: 10.1124/mol.112.081182
This article has not been copyedited and formatted. The final version may differ from this version.

Introduction:

Seven-transmembrane G protein-coupled receptors (GPCRs) are the single largest family of receptors localized to the cell surface and the most common target for currently available therapeutics (Jacoby, 2006). These receptors are defined by their ability to activate heterotrimeric guanine nucleotide binding proteins upon agonist stimulation. GPCRs without an identified endogenous ligand are considered "orphan receptors" and represent novel therapeutic targets. One such orphan receptor, G protein-coupled receptor 18 (GPR18), is found at high levels in the testis, small intestines and cells associated with the immune system including lymphocytes, thymus and spleen (Gantz et al., 1997).

Recently, N-arachidonyl glycine (NAGly) was identified as the endogenous ligand for GPR18 (Kohno et al., 2006). NAGly is a lipoamino acid found most abundantly in the spinal cord and brain (Huang et al., 2001). The chemical structure of NAGly is similar to that of anandamide (N-arachidonylethanolamide, AEA), but NAGly shows no activity at the two identified cannabinoid receptors, CB_1 and CB_2 (Huang et al., 2001). Anandamide and abnormal cannabidiol (Abn-Cbd), a synthetic cannabinoid, show agonist activity in GPR18-expressing cells (McHugh et al., 2010; McHugh et al., 2012). Interestingly, anandamide exerts vasodilatory effects independent of CB_1- and CB_2R activity (Jarai et al., 1999), suggesting the existence of a third member of the cannabinoid receptor family, possibly GPR18 (McHugh et al., 2010).

GPR18 coupling to pertussis toxin-sensitive $G\alpha_{i/o}$ proteins has been suggested in studies using cell line expression systems (Kohno et al., 2006; McHugh et al., 2010; McHugh et al., 2012; Takenouchi et al., 2012). However, a high-throughput screening of orphan GPCRs and lipid ligands failed to detect activation of GPR18 by NAGly (Yin et

Molecular Pharmacology Fast Forward. Published on October 25, 2012 as DOI: 10.1124/mol.112.081182
This article has not been copyedited and formatted. The final version may differ from this version.

al., 2009). This discrepancy could arise from the different assays used to detect G protein activation. The PathHunter™ assay used by Yang's group assesses G protein-coupling using β-arrestin-mediated internalization, which is a common but not universal desensitization pathway for GPCRs. The MAPK phosphorylation assay used by Bradshaw's group is a distant downstream effector of GPCR activation that can also be activated by multiple types of receptors (e.g. tyrosine kinase receptors). Here, we further examine the G protein signaling pathways of GPR18. We utilized rat superior cervical ganglion neurons to heterologously express GPR18 for study and measured inhibition of Ca^{2+} current as an assay for G protein activation. $G\alpha_{i/o}$ protein-coupled receptor modulation of Ca^{2+} channels is mediated directly by liberated $G\beta\gamma$ (Herlitze et al., 1996; Ikeda, 1996) and occurs within a time course that can be observed during an electrophysiology experiment. The system is robust—to our knowledge, all $G\alpha_{i/o}$-coupled GPCRs that traffic to the plasma membrane produce a Ca^{2+} current inhibition when activated with a cognate agonist.

Surprisingly, we found a lack of GPR18 activation by NAGly and other proposed agonists including anandamide and abnormal cannabidiol. Other commonly associated downstream effectors of $G\alpha_{i/o}$ protein-coupled receptors were examined and no response to NAGly in GPR18-expressing cells was observed. This study brings into question the identity of the endogenous ligand for GPR18 and the renaming of these receptors to the NAGly-receptor.

Molecular Pharmacology Fast Forward. Published on October 25, 2012 as DOI: 10.1124/mol.112.081182
This article has not been copyedited and formatted. The final version may differ from this version.

Materials and Methods:

Molecular cloning and mutagenesis

Oligonucleotide primers for cloning were designed based on NM_182806.1 (*Mus musculus* GPR18 RefSeq accession number) and commercially synthesized (IDT, Coralville, IA). GPR18 was amplified from marathon-ready mouse brain cDNA (Clontech, Mountain View, CA) using PCR and *PfuUltra*™ DNA polymerase (Stratagene, La Jolla, CA). To subclone into the mammalian expression vector pCI (Promega, Madison, WI), we used the following primers: forward 5' – GATCGAATT CACCATGGCC ACCCTGAGCA ATCACAACC – 3' (EcoRI site underlined) and reverse 5' – GATCGATCGC GGCCGCTCAA AGCATCTCAC TGTTCATGTT GC – 3' (NotI site underlined). A fusion construct with GPR18 and enhanced green fluorescent protein (EGFP) was designed with the following primer set: forward 5' – GATCCAAGCT TTGACCATGG CCACCCTGAG CAATCAC – 3' (HindIII site underlined) and reverse 5' – GATCGATCCC GCGGAAGCAT CTCACTGTTC ATGTTGC – 3' (SacII site underlined), and subcloned into EGFP-N1 (Clontech). A cloning error was detected within the junction of the GPR18-EGFP construct that caused a frameshift mutation and dim expression of EGFP. QuikChange™ (Stratagene) site-directed mutagenesis using the following primers, forward 5' – GCAACATGAA CAGTGAGATG CTT*GATATC*C CGCGGGCCCG GGATCC – 3' and reverse 5' – GGATCCCGGG CCCGCGG*GAT ATC*AAGCATC TCACTGTTCA TGTTGC – 3' (SacII site underlined, EcoRV site italicized), were used to return the EGFP sequence in-frame and introduce an EcoRV restriction site. Hemagglutinin (HA)-tagged versions of GPR18 were produced from custom-designed vectors built on a pcDNA3.1+ backbone.

Molecular Pharmacology Fast Forward. Published on October 25, 2012 as DOI: 10.1124/mol.112.081182
This article has not been copyedited and formatted. The final version may differ from this version.

GPR18 was subcloned into a N-terminal 3xHA-tagging vector with the following primers: forward 5' – GCCACCCTGA GCAATCAC – 3' and reverse 5' - GATCGATCGC GGCCGCTCAA AGCATCTCAC TGTTCATGTT GC – 3' (NotI site underlined), using EcoRV and NotI restriction enzymes. A C-terminal 3xHA-tagged construct of GPR18, GPR18-3xHA, was produced by cutting and subcloning from the GPR18-EGFP construct with HindIII and EcoRV. Point mutations of GPR18 and the α_{2A}-adrenergic receptor (ADRA2A) were generated using QuikChange™ site-directed mutagenesis and the primers listed in Table 1. All generated constructs were confirmed by DNA sequencing (Supplemental Figure 1A and B, Macrogen, Rockville, MD).

Live- and fixed-cell staining

HeLa cells (ATCC, Manassas, VA) were cultured (2.0×10^4 cells per mL) in minimal essential medium supplemented with 10% fetal bovine serum, 100 U/mL penicillin and 100 µg/mL streptomycin (MEM+/+, Gibco, Grand Island, NY) on poly-L-lysine coated glass-bottomed dishes (MatTek, Ashland, MA). Cells were transfected with a mixture of 0.5 µg cDNA and 7 µL fully deacylated polyethylenimine (PEI) at 7.5 mM in 100 µL MEM-/- overnight.

For live-cell staining, dishes were gently washed with Dulbecco's phosphate buffered saline with Ca^{2+} and Mg^{2+} (DPBS+/+) to remove culture medium before a blocking solution, 2% BSA in DPBS+/+, was added for 30 min at 37°C. HeLa cells were then incubated with primary antibody (biotin labeled anti-HA.11 clone 16B12, 1:200, Covance, Berkeley, CA) in blocking solution for 1 h at 37°C. After gentle washing of cells with blocking solution, a streptavidin conjugated to quantum dot 655 (Qdot®655)

Molecular Pharmacology Fast Forward. Published on October 25, 2012 as DOI: 10.1124/mol.112.081182
This article has not been copyedited and formatted. The final version may differ from this version.

secondary antibody (1:200, Molecular Probes, Eugene, OR) was added for 1 h at 37°C. Cells were washed with blocking solution for 10 min and then exchanged for DPBS+/+ before imaging.

For immunocytochemistry, dishes were gently washed with DPBS+/+ before fixing with 4% paraformaldehyde for 20 min at room temperature (RT). After washing out fixative with DPBS+/+, HeLa cells were permeabilized with 0.5% Tween-20 in DPBS+/+ for 30 min at RT. Following solution exchange with DPBS+/+, a blocking solution, 2% BSA in Tris buffered saline with 0.05% Tween-20 (TBS-T, 10 mM Tris base, 250 mM NaCl, pH 7.5), was added for 1 h at RT. Primary antibody (biotin anti-HA, 1:500, Covance) in blocking solution was incubated with cells overnight at +4°C. After washing cells with TBS-T for 10 min, secondary antibody (streptavidin Qdot®655, 1:500, Molecular Probes) incubation was for 2 h at RT. Cells were washed with TBS-T for 10 min and then exchanged for DPBS+/+ before imaging.

All staining experiments included parallel negative controls, which received the same treatment except without primary antibody incubation.

Imaging

HeLa cells and neurons expressing EGFP-constructs were imaged using a 63x (1.2 NA) or 40x (1.2 NA) objective mounted on a Zeiss LSM510 Meta confocal microscope with ZEN 2008 acquisition software (Carl Zeiss, Jena, Germany). For EGFP fluorescence, the excitation wavelength was 488 nm and emission wavelength was band-pass filtered between 500 and 550 nm. Qdot®655 fluorescent images were acquired with 488 nm excitation and a 650 and 710 nm band-pass filtered emission.

Molecular Pharmacology Fast Forward. Published on October 25, 2012 as DOI: 10.1124/mol.112.081182
This article has not been copyedited and formatted. The final version may differ from this version.

Western blotting

Unless otherwise indicated, all reagents for Western blotting were from Thermo Scientific (Rockford, IL). Transfected HeLa cells were lysed with Mammalian Protein Extraction Reagent (M-PER) with protease inhibitors for 5 min at RT. A reducing SDS loading buffer was added to lysates and heated, 85°C for 5 min, before electrophoresing samples on a 4-15% Tris-glycine precast gel (Bio-Rad, Hercules, CA) with Laemmli running buffer (Laemmli, 1970). Proteins were transferred to a PVDF membrane at 280 mA for 1 h. The membrane was blocked with 5% BSA in TBS-T for 3 h before incubating overnight with a mouse anti-GFP antibody (1:2000, UC Davis/NIH NeuroMab Facility, Davis, CA) at +4°C. A goat anti-mouse HRP-conjugated secondary antibody (1:1000, 1 h) in blocking solution was applied before chemiluminescent detection of blots with SuperSignal West Femto substrate and a Kodak Image Station 4000R (Carestream Molecular Imaging, Woodbridge, CT). Membranes were stripped with Restore PLUS stripping buffer and reprobed for loading controls. Rabbit anti-tubulin (1:2000, overnight, Cell Signaling, Boston, MA) and rabbit anti-cyclophilin B (1:5000, overnight, Abcam, Cambridge, MA) primary antibodies were used, followed by a goat anti-rabbit HRP-conjugated secondary antibody (1:1000, 1h) and chemiluminescent detection.

Superior cervical ganglion (SCG) neuron dissociation and intranuclear microinjection of cDNA

Molecular Pharmacology Fast Forward. Published on October 25, 2012 as DOI: 10.1124/mol.112.081182
This article has not been copyedited and formatted. The final version may differ from this version.

All animal studies were conducted in accordance with the National Institutes of Health's *Guidelines for Animal Care and Use*.

SCG neurons from adult (6-12 week old) male Wistar rats were dissected and dissociated as described previously (Ikeda, 2004; Ikeda and Jeong, 2004). Briefly, animals were anesthetized by CO_2 inhalation and decapitated before dissection. Two SCG per rat were removed, desheathed, cut into small pieces, and incubated in modified Earles' balanced salt solution (EBSS) containing 2 mg/mL collagenase (CLS4; Worthington Biochemical, Lakewood, NJ), 0.6 mg/mL trypsin (Worthington Biochemical) and 0.1 mg/mL DNase I at 36°C for 1 hour in a water bath shaker oscillating at 110 rpm. The EBSS was supplemented with 3.6 g/L D-glucose and 10 mM HEPES. After incubation, neurons were mechanically dissociated by vigorously shaking the flask for 10 s. Neurons were centrifuged at 570 rpm for 6 min and resuspended in MEM+/+ twice before being plated on poly-L-lysine coated tissue culture dishes. Cells were maintained in a humidified 95% air/5% CO_2 incubator at 37°C.

Three to six hours after dissociation, plasmid constructs were injected directly into the nucleus of SCG neurons as described previously (Ikeda, 2004; Ikeda and Jeong, 2004; Lu et al., 2009). Briefly, cDNA was injected with an Eppendorf FemtoJet microinjector and 5171 micromanipulator (Eppendorf) using an injection pressure and duration of 140-160 hPa and 0.3 s, respectively. Injected plasmids were diluted in EB buffer (10 mM Tris-HCl, pH 8.5) and centrifuged in capillary tubes at 10000 rpm for at least 30 min. GPR18 constructs were injected at a concentration of 50-100 ng/μL and ADRA2A mutants were injected at a lower concentration (10 ng/μL). To identify successfully injected neurons, pEGFP-N1 cDNA (Clontech) was co-injected at a

Molecular Pharmacology Fast Forward. Published on October 25, 2012 as DOI: 10.1124/mol.112.081182
This article has not been copyedited and formatted. The final version may differ from this version.

concentration of 5 ng/µl. Following injections, neurons were incubated overnight at 37°C and electrophysiological experiments were performed the following day.

Electrophysiology

Ca^{2+}-channel currents (I_{Ca}) and G protein-coupled inwardly rectifying K^+ currents (I_{GIRK}) were recorded using conventional whole-cell patch-clamp techniques (Hamill et al., 1981). Patch electrodes were pulled from borosilicate glass capillaries (1.65 mm outer diameter, 1.20 mm inner diameter, King Precision Glass, Claremont, CA) using a Model P-97 micropipette puller (Sutter Instrument, Novato, CA). The patch electrodes were coated with silicone elastomer (Sylgard 184, Dow Corning, Midland, MI) and fire-polished. A Ag/AgCl pellet connected to the bath solution via a 0.15 M NaCl/agar bridge was used as a ground. The cell membrane capacitance was cancelled and series resistance was compensated (>85% prediction and correction; lag set to 5 µs) with a patch-clamp amplifier (Axopatch 200A/B, Molecular Devices, Sunnyvale, CA). Voltage protocol generation and data acquisition were performed using custom-designed software (S5) on a Macintosh G4 computer (Apple, Cupertino, CA). Current traces were filtered at 2 kHz (−3 dB; 4-pole Bessel), digitized at 10 kHz with a 16-bit analog-to-digital converter board (ITC-18, HEKA, Bellmore, NY) and stored on the computer for later analyses.

For recording I_{Ca}, patch pipettes were filled with an internal solution containing (in mM) 120 N-methyl-D-glucamine, 20 tetraethylammonium hydroxide (TEA-OH), 11 EGTA, 10 HEPES, 10 sucrose, 1 $CaCl_2$, 14 Tris-creatine phosphate, 4 MgATP and 0.3 Na_2GTP, pH 7.2 with methanesulfonic acid. External I_{Ca} recording solution consisted of (in mM) 140 methanesulfonic acid, 145 TEA-OH, 10 HEPES, 10 glucose, 10 $CaCl_2$ and

Molecular Pharmacology Fast Forward. Published on October 25, 2012 as DOI: 10.1124/mol.112.081182
This article has not been copyedited and formatted. The final version may differ from this version.

0.0003 tetrodotoxin (TTX), pH 7.4 with TEA-OH. A Tris-based external I_{Ca} solution was also tested containing (in mM) 155 Tris-base, 20 HEPES, 10 glucose, 10 $CaCl_2$ and 0.0003 TTX, pH 7.4 with methanesulfonic acid.

To measure G protein modulation of Ca^{2+}-channels, a double-pulse protocol consisting of two 25 ms test pulses to +10 mV separated by a 50 ms conditioning pulse to +80 mV (Elmslie et al., 1990) was evoked every 10 s from a holding potential of -80 mV. To measure low- and high-voltage activated (LVA and HVA)-I_{Ca} in the same cell, two 25 ms pulses, the first to -40 mV and the second to +10 mV, separated by a 60 ms pulse to -60 mV, to inactivate LVA-I_{Ca}, was applied every 10 s from a holding potential of -80 mV. I_{Ca}-voltage relationships were studied by applying a series of 70 ms depolarizing voltage steps from a holding potential of -80 mV.

For recording I_{GIRK}, patch pipettes were filled with an internal solution containing (in mM) 135 KCl, 11 EGTA, 10 HEPES, 2 $MgCl_2$, 1 $CaCl_2$, 4 MgATP and 0.3 Na_2GTP, pH 7.2 with KOH. External I_{GIRK} recording solution consisted of (in mM) 140 NaCl, 5.4 KCl, 10 HEPES, 15 glucose, 15 sucrose, 2 $CaCl_2$, 0.8 $MgCl_2$ and 0.0003 TTX, pH 7.4 with NaOH.

I_{GIRK} were elicited from 200 ms voltage ramps from -140 to -40 mV and the holding potential was set to -60 mV.

Live-cell bioluminescence resonance energy transfer (BRET)-based assay for cyclic adenosine monophosphate (cAMP)

Human embryonic kidney (HEK)-293 cells (ATCC) were plated (5.0×10^5 cells per mL) on 24-well plates in MEM+/+. Cells were transfected overnight with a mixture

Molecular Pharmacology Fast Forward. Published on October 25, 2012 as DOI: 10.1124/mol.112.081182
This article has not been copyedited and formatted. The final version may differ from this version.

of 150 ng CAMYEL cDNA (Jiang et al., 2007), 100 ng empty vector or selected G protein-coupled receptor cDNA and 4 μL PEI in 50 μL MEM-/- per well. Approximately 16 h post-transfection, HEK cells were removed from 24-well plates with TrypLE Express (Gibco) and washed twice in DPBS+/+ before loading onto black 96-well microplates (Berthold, Bad Wildbad, Germany).

Light intensity was measured using a Tristar LB941 luminometer (Berthold) controlled by MikroWin 2000 acquisition software (Berthold). Net BRET was calculated from the light intensity measured alternately from donor and acceptor channels in 1 s intervals using the emission filters 460/60 nm and 542/27 nm, respectively (Semrock, Rochester, NY). For testing the kinetic responses of GPCRs coupled to $G\alpha_{i/o}$ pathways, 14 s of baseline recording, followed by injection of 5 μM h-coelenterazine (Nanolight Technology, Pinetop, AZ) substrate, 120 s of recording, injection of 1 μM forskolin, 240 s of recording, injection of agonist (10 μM NAGly or 100 μM glutamate) and 540 s of recording. For testing the kinetic responses of GPCRs coupled to $G\alpha_s$ pathways, 14 s of baseline recording, followed by injection of 5 μM h-coelenterazine, 120 s of recording, injection of agonist (10 μM NAGly or 10 μM dopamine), 240 s of recordings, injection of 10 μM forskolin and 240 s of recording.

Drugs and chemicals

Unless otherwise stated, all chemicals were purchased from Sigma-Aldrich. TTX was purchased from Alomone Laboratories (Jerusalem, Israel); pertussis toxin (PTX) and cholera toxin (CTX) were purchased from List Biological Laboratories (Campbell, CA); N-arachidonyl glycine (NAGly), N-arachidonoyl-L-serine (ARA-S), anandamide (AEA),

Molecular Pharmacology Fast Forward. Published on October 25, 2012 as DOI: 10.1124/mol.112.081182
This article has not been copyedited and formatted. The final version may differ from this version.

abnormal cannabidiol (Abn-Cbd) and O-1602 were purchased from Cayman Chemical (Ann Arbor, MI); h-coelenterazine was purchased from Nanolight Technology (Pinetop, AZ), dopamine hydrochloride was purchased from Tocris (Bristol, UK). PTX or CTX was added (0.5 μg/ml) to the culture medium bathing SCG neurons or HEK cells during overnight incubation (>16 h).

Drugs for electrophysiological experiments were diluted to final concentrations from stock solutions on the day of experiment and applied directly onto neurons using a custom-made gravity-fed perfusion system with separate perfusion lines feeding into a 4-bore glass capillary tube (VitroCom, Mountain Lakes, NJ) connected to a fused silica capillary tube. A constant flow of external solution was applied onto cells during baseline recordings and switched to a drug solution during drug applications to avoid flow-induced artifacts. All recordings were performed at room temperature (20-24°C).

For BRET experiments, drugs were injected into each well by the luminometer's injection system. Before the start of experiments, all lines were primed with distilled water and then re-primed with the drug solution to be injected. Chemicals were made the day of experiments at a concentration so the total volume (injected volume + volume in well) would produce the final desired concentration.

Data analysis and statistical testing

ImageJ software (v.1.45I, NIH, Bethesda, MD) was used to analyze and adjust contrast of images for presentation in figures. Igor Pro version 6 (WaveMetrics, Portland, OR) was used to analyze current traces. I_{Ca} amplitude was measured isochronally 10 ms after the initiation of a test pulse to +10 mV or at the maximum peak I_{Ca} during test

Molecular Pharmacology Fast Forward. Published on October 25, 2012 as DOI: 10.1124/mol.112.081182
This article has not been copyedited and formatted. The final version may differ from this version.

pulses to -40 mV. The facilitation ratio (FR) was determined as the ratio of postpulse to prepulse I_{Ca}. The peak I_{GIRK} was taken 3 ms after the start of the ramp. Drug responses were normalized to baseline I_{Ca} or I_{GIRK} using the equation $I_{drug}/I_{baseline}$ x 100, where I_{drug} and $I_{baseline}$ are the current amplitudes during and before drug application, respectively. Net BRET was calculated as $A/D - d$, where A is the acceptor channel intensity, D is the donor channel intensity and d is the background or spectral overlap (calculated previously as the A/D for donor, Rluc8, alone). A single net BRET value, 4 min following injection of agonist, was used for comparison of net BRET values between groups.

Statistical tests were performed with GraphPad Prism 5 for Mac OS X (GraphPad Software, La Jolla, CA). Individual data points were represented on graphs with the mean ± SEM. Statistical significance between two groups was determined using an unpaired Student's *t* tests. To compare three or more groups, a one-way analysis of variance (ANOVA) test followed by Newman-Keuls post-test was performed. $P < 0.05$ was considered statistically significant, except when a multiple comparison Bonferroni correction was applied as indicated.

Molecular Pharmacology Fast Forward. Published on October 25, 2012 as DOI: 10.1124/mol.112.081182
This article has not been copyedited and formatted. The final version may differ from this version.

Results:

Heterologous expression of full-length GPR18 at the membrane

To determine the cellular localization of heterologously expressed receptor, GPR18-EGFP cDNA was injected into SCG neurons and compared with injected EGFP and EGFP-KRas tail cDNA expression, which label the cytoplasm and plasma membrane of the cell, respectively. The GPR18 construct displayed a “rim-like” fluorescence (Figure 1A, top panel). This pattern was unlike cytoplasmic EGFP (Figure 1B, top panel) but similar to membrane-bound EGFP-KRas tail (Figure 1C, top panel). Line plots of fluorescence intensity (Figure 1A-C, top panel insets) show the highest intensity values along the edge of neurons injected with GPR18-EGFP or EGFP-KRas tail, whereas fluorescence intensities of EGFP-injected SCG neurons were uniform across the cell. HeLa cells were also transfected with EGFP-labeled constructs to compare expression in a cell line expression system (Figure 1A-C, bottom panels). In expressing HeLa cells, GPR18-EGFP and EGFP-KRas tail displayed a “rim-like” fluorescence pattern and EGFP displayed fluorescence throughout the cell, similar to SCG neuron expression.

Western blotting was used to confirm expression of full-length GPR18. An antibody against GFP was used to detect EGFP-tagged receptor because commercially available antibodies for GPR18 have not been validated against a GPR18-knock-out animal. An approximately 80 kD band was detected in the GPR18-EGFP lane (Figure 1D). This band is larger than the predicted size of the protein, 66 kD, which suggests post-translational modification of the receptor. The GFP antibody also detected EGFP and EGFP-KRas tail constructs and their bands corresponded to the predicted protein mass, 27 and 29 kD, respectively. The same blot was reprobed for loading controls

Molecular Pharmacology Fast Forward. Published on October 25, 2012 as DOI: 10.1124/mol.112.081182
This article has not been copyedited and formatted. The final version may differ from this version.

α-tubulin and cyclophilin B, which corresponded to bands of 51 and 19 kD, respectively (Figure 1E).

To confirm GPR18 expression in the plasma membrane, live-cell staining of epitope-tagged GPR18 was performed. The perimeter of HeLa cells expressing the external epitope-tagged version of GPR18, 3xHA-GPR18, was stained following the live-cell staining procedure (see Methods, Figure 2A), whereas staining was absent in HeLa cells expressing the internal epitope-tagged version of GPR18, GPR18-3xHA (Figure 2B). To confirm expression of receptors, GPR18-3xHA-expressing cells were stained following fixation and permeabilization to allow antibody access to the interior of cells. Fixed and permeabilized GPR18-3xHA cells stained positive for the HA-epitope along the edge and within HeLa cells (Figure 2C). Staining was absent in negative controls (data not shown).

Taken together, heterologously expressed GPR18 inserts with appropriate topology into the plasma membrane where it is accessible to agonists and G proteins.

Direct potentiation of HVA-Ca^{2+} channels by NAGly but no GPR18-mediated inhibition of I_{Ca} by NAGly

To study coupling of GPR18 to G proteins, we used sympathetic neurons as a heterologous expression system. We have expressed non-native GPCRs in SCG neurons by intranuclear microinjection (Ikeda, 2004; Ikeda and Jeong, 2004; Lu et al., 2009) or RNA transfection (Williams et al., 2010) and reliably recapitulated endogenous G protein signaling pathways for study (Guo and Ikeda, 2004; Guo and Ikeda, 2005; Guo et al., 2008b; Ikeda et al., 1995). Furthermore, we can examine G protein activity in SCG

Molecular Pharmacology Fast Forward. Published on October 25, 2012 as DOI: 10.1124/mol.112.081182
This article has not been copyedited and formatted. The final version may differ from this version.

neurons by measuring GPCR-mediated inhibition of endogenous Ca^{2+} current (I_{Ca}). We have previously shown Ca^{2+}-channels in SCG neurons are modulated by GPCRs coupled through various G protein families: $G\alpha_{i/o}$ (Guo and Ikeda, 2004; Guo and Ikeda, 2005; Ikeda, 1992; Ikeda et al., 1995; Ikeda et al., 1987; Zhu and Ikeda, 1993), including $G\alpha_z$ (Jeong and Ikeda, 1998), $G\alpha_s$ (Zhu and Ikeda, 1994) and $G\alpha_{q/11}$ (Kammermeier et al., 2000).

We first examined the effect of N-arachidonyl glycine (NAGly) application on I_{Ca} recorded from uninjected neurons. I_{Ca} was evoked at 0.1 Hz using a double-pulse voltage protocol (Figure 3Ai, inset) in solutions designed to isolate I_{Ca}. The facilitation ratio (FR, ⊡), defined as the ratio of I_{Ca} evoked in the second test pulse (postpulse, Figure 3, ●) to I_{Ca} in the first test pulse (prepulse, Figure 3, ○), was used as a measure of Gβγ-mediated I_{Ca} modulation. NAGly (10 μM) potentiated I_{Ca} (Figure 3Ai), increasing both pre- and postpulse I_{Ca} resulting in no change in the FR (Figure 3Aii and 3Aiii). A lower concentration of NAGly (1 μM) did not produce a change in I_{Ca}. As a positive control for G protein activation, norepinephrine (NE, 10 μM) was applied to the same uninjected neuron. NE, activating endogenous α_2-adrenergic receptors, produced a robust decrease in I_{Ca} and an increase in the FR (Figure 3Aii and 3Aiii). Our lab has previously documented a direct effect of lipoamino acids on voltage-gated Ca^{2+} channels (Guo et al., 2008a). Here, we reproduced the result of enhanced I_{Ca}, in a voltage-dependent manner, and a hyperpolarized I_{Ca}-voltage curve with NAGly (Figure 3B). NAGly had a similar effect on untagged GPR18-expressing SCG neurons as uninjected controls (Figure 3C). A lower dose of NAGly (1 μM) produced no change in I_{Ca}, and a higher dose increased I_{Ca} (Figure 3Ci) both pre- and postpulse currents (Figure 3Cii) with no change in FR (Figure

Molecular Pharmacology Fast Forward. Published on October 25, 2012 as DOI: 10.1124/mol.112.081182
This article has not been copyedited and formatted. The final version may differ from this version.

3Ciii). NE-mediated inhibition of I_{Ca} persisted in untagged GPR18-expressing neurons (Figure 3Cii and 3Ciii). Drug responses, expressed as I_{Ca} amplitude during drug application normalized to baseline I_{Ca}, were compared between both groups in Figure 3D. Responses to low or high concentrations of NAGly were not significantly different between uninjected controls and untagged GPR18-expressing neurons (unpaired t-test, *p>0.05*). NE responses were also not significantly different between uninjected controls and untagged GPR18-expressing neurons (unpaired t-test, *p>0.05*). In every cell tested, both concentrations of NAGly failed to inhibit I_{Ca}, whereas all exhibited NE-mediated inhibition of I_{Ca}. The enhancement of I_{Ca} by NAGly was not mediated by endogenous $G\alpha_{i/o}$ protein-coupled receptors since overnight incubation of uninjected and untagged GPR18-injected SCG neurons with pertussis toxin (PTX), which uncouples $G\alpha_{i/o}$ protein signaling from GPCRs, did not affect NAGly responses. Following PTX treatment, NAGly still potentiated I_{Ca} in uninjected SCG neurons (106.9 ± 2.3% baseline I_{Ca}, n = 8) and untagged GPR18-expressing SCG neurons (112.4 ± 9.7% baseline I_{Ca}, n = 3).

NAGly and NE responses were also tested in N- and C-terminal tagged versions of GPR18. I_{Ca} were potentiated by NAGly 114.6 ± 5.7% (n = 7), 105.1 ± 1.6% (n = 7) and 105.1 ± 2.8% (n = 5) from baseline I_{Ca} in GPR18-EGFP-, 3xHA-GPR18- and GPR18-3xHA-expressing neurons, respectively. NE inhibited I_{Ca} 41.3 ± 3.7%, 43.1 ± 4.5% and 42.9 ± 5.1% of baseline I_{Ca} in GPR18-EGFP-, 3xHA-GPR18- and GPR18-3xHA-injected neurons, respectively. No significant difference in NAGly or NE responses was observed between untagged and tagged versions of GPR18 (one-way ANOVA, *p>0.05*). Untagged GPR18 was heterologously expressed in cells for the rest of this study, unless otherwise stated.

Molecular Pharmacology Fast Forward. Published on October 25, 2012 as DOI: 10.1124/mol.112.081182
This article has not been copyedited and formatted. The final version may differ from this version.

Inhibition of low-voltage activated, LVA, Ca^{2+} channels by NAGly (Barbara et al., 2009) was used as a positive control for agonist activity. SCG neurons do not endogenously express T-type Ca^{2+} channels (Figure 4A), so we injected cDNA encoding $Ca_v3.1$ or $Ca_v3.2$ into cells. LVA-I_{Ca} elicited by a test pulse to -40 mV (Figure 4A, inset) was transiently activated showing fast inactivation during the 25 ms pulse (Figure 4B). Currents were also reversibly inhibited by application of 100 μM Ni^{2+} (Ni^{2+} inhibition of $Ca_v3.1$-expressing neurons = 17 ± 4.5% baseline I_{Ca}, n = 5; Ni^{2+} inhibition of $Ca_v3.2$-expressing neurons = 9.0 ± 1.1% baseline I_{Ca}, n = 5). NAGly applied to $Ca_v3.1$-injected SCG neurons inhibited LVA-I_{Ca} whilst potentiating HVA-I_{Ca} (Figure 4B). In SCG neurons injected with $Ca_v3.2$, NAGly-induced inhibition of LVA-I_{Ca} (64.1 ± 4.8% baseline I_{Ca}, n = 3) and potentiated HVA-I_{Ca} (106.1 ± 10.6% baseline I_{Ca}, n = 3). In SCG neurons co-injected with $Ca_v3.1$ and GPR18, NAGly inhibited LVA-I_{Ca} and potentiated HVA-I_{Ca} (Figure 4C). In cells injected with $Ca_v3.2$ and GPR18, NAGly inhibited LVA-I_{Ca} (52.1 ± 7.6% baseline I_{Ca}, n = 8) and potentiated HVA-I_{Ca} (109.3 ± 7.8% baseline I_{Ca}, n = 8). No significant difference in NAGly inhibition of LVA-I_{Ca} was observed between $Ca_v3.1$-expressing neurons with or without GPR18 co-expressed (Figure 4D, unpaired t-test, $p>0.05$). NAGly enhancement of HVA-I_{Ca} was also not significantly different between $Ca_v3.1$ alone and $Ca_v3.1$ with GPR18-expressing neurons (Figure 4D unpaired t-test, $p>0.05$).

To ensure the external recording solution was not interfering with drug activity at the receptor, a Tris-based external I_{Ca} solution was also tested. No significant difference in NAGly responses was observed between uninjected and GPR18-expressing SCG neurons (for controls, 122.4 ± 3.2% baseline I_{Ca}, n = 9; for GPR18-expressing neurons,

Molecular Pharmacology Fast Forward. Published on October 25, 2012 as DOI: 10.1124/mol.112.081182
This article has not been copyedited and formatted. The final version may differ from this version.

115.5 ± 2.2% baseline I_{Ca}, n = 10; unpaired t-test, *p>0.05*) or NE responses (for controls, 44.1 ± 4.2%, n = 9; for GPR18-expressing neurons, 40.8 ± 2.7%, n = 10, unpaired t-test, *p>0.05*).

Although a positive effect from GPR18 has been observed from mouse-dervied cell lines endogenously expressing GPR18 (Burstein et al., 2011; McHugh et al., 2010; Takenouchi et al., 2012), most GPR18 studies have utilized human GPR18 (Gantz et al., 1997; Kohno et al., 2006; McHugh et al., 2012; Qin et al., 2011). To assess the variability of GPR18 across species, protein sequences from different species were analyzed by protein alignment. Based on GPR18 protein sequence alignment (Supplemental Figure 1C), mouse GPR18 is 95.2% identical, 97% similar to rat GPR18 and 85.8% identical, 92.1% similar to human GPR18. The greatest divergence in GPR18 protein appears in the N-terminus. Since the sequences are highly similar in the transmembrane domains and important signaling regions of GPCRs, we are confident our mouse GPR18 clone is comparable to studies of human GPR18. Also, since mouse and rat GPR18 protein sequences are highly similar, we do not anticipate difficulty heterologously expressing the mouse GPR18 clone in rat neurons.

Thus, we only observed direct effects of NAGly on LVA-I_{Ca} and HVA-I_{Ca} that are not G protein mediated. Furthermore, we did not observe NAGly-mediated inhibition of HVA-I_{Ca} in GPR18-injected neurons.

Other potential agonists of GPR18 do not inhibit I_{Ca}

Other proposed agonists of GPR18 were tested on SCG neurons expressing GPR18 and inhibition of I_{Ca} was used as a measure of G protein activation (Figure 5). N-

Molecular Pharmacology Fast Forward. Published on October 25, 2012 as DOI: 10.1124/mol.112.081182
This article has not been copyedited and formatted. The final version may differ from this version.

arachidonoyl-L-serine (ARA-S, 10 μM), another lipoamino acid, potentiated I_{Ca} in all groups tested: uninjected, GPR18- and CB_1R-expressing SCG neurons. No significant difference between groups was observed (one-way ANOVA, $p>0.05$). Anandamide (AEA, 10 μM), the endocannabinoid neurotransmitter, did not inhibit I_{Ca} in uninjected or GPR18-injected cells. AEA inhibited I_{Ca} in CB_1R expressing neurons, which was significantly different from all groups (one-way ANOVA, $p<0.05$). Synthetic cannabinoids, abnormal cannabidiol and O-1602, had no effect on baseline I_{Ca} in uninjected or GPR18-expressing neurons. NE was applied to all cells as a positive control for G protein modulation and found to inhibit I_{Ca}. NE responses from CB_1R-injected neurons are significantly less than the other groups tested (one-way ANOVA, $p<0.001$), possibly due to the over-expression of exogenous receptor and sequestration of available G proteins from other GPCRs.

Mutations in GPCRs that induce tonic receptor activity do not activate GPR18

To by-pass the need for agonists to activate GPR18, mutations that induce constitutive activity of receptors were introduced. These mutations were based on mutagenesis studies of the α_{1B}-adrenergic receptor (Cotecchia et al., 1990; Kjelsberg et al., 1992; Scheer et al., 1996; Scheer et al., 1997) as illustrated in Supplementary Figure 2 with snake plot diagrams (Supplementary Figure 2A) and sequence alignments (Supplementary Figure 2B). Site-directed mutagenesis and primers listed in Table 1 were used to generate mutants of GPR18 and a $G\alpha_{i/o}$ protein-coupled receptor, the α_{2A}-adrenergic receptor or ADRA2A.

Molecular Pharmacology Fast Forward. Published on October 25, 2012 as DOI: 10.1124/mol.112.081182
This article has not been copyedited and formatted. The final version may differ from this version.

The properties of I_{Ca} inhibition induced by constitutively active $G\alpha_{i/o}$-coupled receptors are analogous to the inhibition induced by agonist application: a high FR and kinetic slowing during prolonged voltage depolarization. Other GPCR responses may also be inhibited by expression of constitutively active receptors since excess free-$G\beta\gamma$ is loaded onto downstream effectors; thus, effectively reducing the dynamic range of $G\beta\gamma$-mediated responses. Constitutively active GPCRs that inhibit I_{Ca} through voltage-independent mechanisms are more difficult to assess since inhibited currents display similar kinetics as uninhibited currents and the mechanisms responsible for I_{Ca} inhibition can be quite diverse. The overall reduction in I_{Ca} amplitude, or I_{Ca} density, may indicate tonic receptor activity for such mechanisms of I_{Ca} inhibition. Thus, basal FR, NE-mediated I_{Ca} inhibition and I_{Ca} density were used as measures of tonic receptor activity.

The D/ERY motif is common in all GPCRs and mutations in the first residue of the motif can induce constitutive activity of receptors (Scheer et al., 1996; Scheer et al., 1997). Expression of a GPR18 version of this mutation, GPR18 D118T-EGFP, was localized primarily in a membrane network inside the cell, reminiscent of the endoplasmic reticulum (ER), and not in the plasma membrane (Figure 6A, left). A substitution mutation of the glutamate residue to alanine, an amino acid that confers less constitutive activity than threonine (Scheer et al., 1997), did not alter expression of the GPR18 mutant from the ER (data not shown). I_{Ca} from GPR18 D118T-expressing neurons was elicited using the double-pulse voltage protocol (Figure 6A, right) and found to be indistinguishable from controls. The increase in I_{Ca} amplitude in the postpulse, following a long depolarizing conditioning pulse, represents relief of basal $G\beta\gamma$-mediated inhibition of I_{Ca} and is responsible for a basal FR >1. The basal FR measured in GPR18

Molecular Pharmacology Fast Forward. Published on October 25, 2012 as DOI: 10.1124/mol.112.081182
This article has not been copyedited and formatted. The final version may differ from this version.

D118T- and GPR18 D118A-injected neurons was similar to uninjected controls (Table 2). NE responses were also similar between GPR18 D118T and uninjected controls (Figure 6A, right and Table 2). In contrast, I_{Ca} measured from SCG neurons expressing ADRA2A D130T had a significantly larger basal FR than its GPR18 mutant counterpart (Table 2, unpaired t-test, $p<0.05$), which was clearly observed with the double-pulse voltage protocol (Figure 6B). The kinetic slowing of I_{Ca} was present during the first test pulse of ADRA2A D130T mutants (Figure 6B). The increased basal FR in ADRA2A D130T mutants was blocked by overnight PTX treatment (ADRA2A D130T basal FR after PTX = 1.3 ± 0.06, n = 7), indicating tonically active ADRA2A receptors coupled to $G\alpha_{i/o}$ proteins.

Mutations in the highly conserved asparagine residue within the first transmembrane domain of GPCRs (Supplementary Figure 2A and B) can also induce constitutive activity (Scheer et al., 1996). In addition, mutations in the C-terminal end of the third intracellular loop have been described for ADRA1B (Cotecchia et al., 1990; Kjelsberg et al., 1992) and ADRA2A (Ren et al., 1993) to induce constitutive activity. Analogous mutations were generated in GPR18 and ADRA2A, based on sequence alignment to ADRA1B (Supplementary Figure 2B) and topographical location (Supplementary Figure 2A), and constitutive activity was assessed. Mutations introduced into GPR18 failed to tonically active receptor as measured by basal FR, NE-response, and I_{Ca} density (Table 2). On the other hand, mutations designed to constitutively activate the ADRA2A receptor produced significantly larger basal FR than similar mutations in GPR18 (Table 2, unpaired t-test with multiple comparison correction, $p<0.017$) and the

Molecular Pharmacology Fast Forward. Published on October 25, 2012 as DOI: 10.1124/mol.112.081182
This article has not been copyedited and formatted. The final version may differ from this version.

ADRA2A N51A mutant significantly reduced the effectiveness of NE-induced inhibition of I_{Ca}.

Thus, mutations predicted to induce constitutive receptor activity did not activate GPR18 but were effective when introduced into ADRA2A receptors, which tonically activate $G\alpha_{i/o}$ signaling pathways.

Proposed GPR18 agonists do not inhibit I_{Ca} in SCG neurons expressing a non-constitutively active mutant of GPR18

A recent study found endogenous GPR18 is constitutively active and differentially expressed in melanoma metastases (Qin et al., 2011). However, we found no indication GPR18 expressed in SCG neurons was constitutively active (basal FR = 1.3 ± 0.04, n = 25; NE-mediated I_{Ca} inhibition = 47.4 ± 3.6% baseline I_{Ca}, n = 17; I_{Ca} density = -25.4 ± 2.2 pA/pF, n = 25). This paper also describes a single amino acid residue responsible for conferring constitutive activity of GPR18 (A108) and mutating the residue to an asparagine restored NAGly-induced G protein signaling. We tested this constitutively active null mutant by monitoring I_{Ca} in SCG neurons during agonist application.

HeLa cells transfected with GPR18 A108N-EGFP displayed a “rim-like” fluorescence pattern (Figure 6C, left). In SCG neurons expressing GPR18 A108N, NAGly potentiated pre- and postpulse I_{Ca} elicited with the double-pulse voltage protocol (Figure 6C, right). Other proposed agonists of GPR18, anandamide and abnormal cannabidiol, were also tested in GPR18 A108N-injected cells but neither induced I_{Ca} inhibition (Figure 6C, lower panel). Only the positive control, NE, produced a significant

Molecular Pharmacology Fast Forward. Published on October 25, 2012 as DOI: 10.1124/mol.112.081182
This article has not been copyedited and formatted. The final version may differ from this version.

reduction in I_{Ca} in GPR18 A108N-expressing neurons (Figure 6D, one-way ANOVA, *$p<0.001$*).

No evidence of GPR18 coupling to $G\alpha_z$

The lack of GPR18 activation by NAGly prompted us to explore possible coupling of GPR18 to other Gα proteins not endogenously expressed in SCG neurons. We have previously expressed $G\alpha_z$ in SCG neurons (Jeong and Ikeda, 1998) and found coupling of $G\alpha_z$ to endogenous GPCRs (Figure 7A). In $G\alpha_z$-expressing cells, NE-induced I_{Ca} inhibition by a Gβγ-mediated mechanism: there was kinetic slowing of I_{Ca} during NE application in the first test pulse (Figure 7Ai), substantial relief of prepulse I_{Ca} inhibition by the conditioning pulse and thus increase in FR during NE application (Figure 7Aiii). The kinetics of NE activation and deactivation in $G\alpha_z$-injected cells (Figure 7Aii) were slower than endogenous $G\alpha_{i/o}$ protein-coupling (Figure 3Aiii), which is consistent with the slower intrinsic GTPase activity of $G\alpha_z$ compared to $G\alpha_i$ or $G\alpha_o$. Together with the persistence of NE-mediated inhibition of I_{Ca} in $G\alpha_z$-expressing neurons after overnight PTX treatment (Figure 7C) suggests coupling of endogenous α_2-adrenergic receptors to $G\alpha_z$.

NAGly slightly potentiated I_{Ca} in $G\alpha_z$-injected SCG neurons (Figure 7Ai), increasing both pre- and postpulse I_{Ca} (Figure 7Aii) resulting in no change of the FR (Figure 7Aiii). In SCG neurons injected with $G\alpha_z$ and GPR18, NE, but not NAGly, induced inhibition of I_{Ca} (Figure 7Bi and 7Bii) and increased the FR during NE application (Figure 7Biii). NAGly responses were not significantly different between uninjected, $G\alpha_z$ alone, GPR18 co-expressing $G\alpha_z$ and GPR18 A108N co-expressing $G\alpha_z$

Molecular Pharmacology Fast Forward. Published on October 25, 2012 as DOI: 10.1124/mol.112.081182
This article has not been copyedited and formatted. The final version may differ from this version.

groups (Figure 7C, one-way ANOVA, *p>0.05*). NE responses in PTX-treated neurons were significantly lower in $G\alpha_z$ alone, GPR18 co-expressing $G\alpha_z$ and GPR18 A108N co-expressing $G\alpha_z$ groups compared to uninjected controls (Figure 7C, one-way ANOVA, *p<0.001*).

Mutants of GPR18 designed to induce constitutive activity were also co-expressed with $G\alpha_z$ to test possible coupling. Basal FR was significantly reduced in SCG neurons expressing $G\alpha_z$ compared to uninjected controls (one-way ANOVA, *p<0.001*), but no significant difference in basal FR was found between the various GPR18 mutants when co-expressed with $G\alpha_z$ (Figure 7Di). NE-induced inhibition of I_{Ca} was also unchanged across all groups tested (Figure 7Dii).

Therefore, we found no evidence of GPR18 coupling to $G\alpha_z$.

No evidence of GPR18 coupling to $G\alpha_{15}$

Potential coupling of GPR18 to $G\alpha_{15}$ was also tested. $G\alpha_{15}$ is highly expressed in hematopoietic cells (Giannone et al., 2010) similar to GPR18 expression. Although $G\alpha_{15}$ is considered a promiscuous G protein, capable of coupling various classes of GPCRs, reconstitution of $G\alpha_{15}$ signaling and functional coupling of this G protein to endogenous GPCRs in SCG neurons has yet to be demonstrated.

To demonstrate functional coupling of a GPCR to $G\alpha_{15}$ in SCG neurons, we used I_{Ca} inhibition as an assay for G protein activity. Expression of $G\alpha_{15}$ alone suppressed endogenous NE-mediated signaling (Supplementary Figure 3A). This artifact of $G\alpha$ protein over-expression, which sequesters available $G\beta\gamma$ protein, could be alleviated by co-injecting $G\beta_1$ and $G\gamma_2$ with $G\alpha_{15}$ to restore the stoichiometric balance of

Molecular Pharmacology Fast Forward. Published on October 25, 2012 as DOI: 10.1124/mol.112.081182
This article has not been copyedited and formatted. The final version may differ from this version.

heterotrimeric G protein signaling (Supplementary Figure 3B). The basal FR of $G\alpha_{15}$ was also restored to uninjected control levels after co-expressing $G\beta_1\gamma_2$ (for $G\alpha_{15}$ alone, basal FR = 1.0 ± 0.01, n = 16; for $G\alpha_{15}\beta_1\gamma_2$, basal FR = 1.3 ± 0.02, n = 36). Endogenous α_2-adrenoceptors do not couple to PTX-insensitive $G\alpha_{15}$ because there was no NE-mediated inhibition of I_{Ca} in $G\alpha_{15}\beta_1\gamma_2$-expressing cells following overnight PTX treatment (Supplementary Figure 3C). Since mGluR2 has been shown to couple to $G\alpha_{15}$ *in vitro* (Gomeza et al., 1996), mGluR2 and $G\alpha_{15}\beta_1\gamma_2$ were co-expressed in SCG neurons and glutamate-induced inhibition of I_{Ca} after PTX treatment was measured (Figure 8A). The properties of I_{Ca} inhibition by mGluR2 coupled to $G\alpha_{15}$ were distinct from mGluR2 coupled to $G\alpha_{i/o}$ (Supplemental Figure 3D and E): there was no kinetic slowing during the first test pulse of the double-pulse protocol, almost equal inhibition of the pre- and postpulse I_{Ca} and therefore smaller change in the FR, and insensitivity to PTX. $G\alpha_{i/o}$-mediated pathways still dominated mGluR2 signaling because glutamate induced a change in FR in cells co-expressing $G\alpha_{15}\beta_1\gamma_2$ and mGluR2 (Supplementary Figure 3F).

In PTX-treated SCG neurons injected with $G\alpha_{15}\beta_1\gamma_2$ and GPR18, NAGly potentiated pre- and postpulse I_{Ca} evoked by the double-pulse voltage protocol (Figure 8Bi and 8Bii), with no change in the FR (Figure 8Biii). No NAGly-induced inhibition of I_{Ca} was observed in PTX-treated SCG neurons co-expressing $G\alpha_{15}\beta_1\gamma_2$ and GPR18 or GPR18 A108N (Figure 8C) and NAGly responses were not significantly different between all groups tested (one-way ANOVA, $p>0.05$). No NE-induced inhibition of I_{Ca} was observed in all PTX-treated groups tested (Figure 8C).

Mutants of GPR18 designed to induce constitutive activity were also co-expressed with $G\alpha_{15}\beta_1\gamma_2$ to test possible coupling. I_{Ca} density was significantly reduced in $G\alpha_{15}\beta_1\gamma_2$

Molecular Pharmacology Fast Forward. Published on October 25, 2012 as DOI: 10.1124/mol.112.081182
This article has not been copyedited and formatted. The final version may differ from this version.

and mGluR2-injected neurons during glutamate application (one-way ANOVA, $p<0.05$) but mutants of GPR18 co-expressed with $G\alpha_{15}\beta_1\gamma_2$ did not change I_{Ca} density compared to uninjected controls (Figure 8D).

Therefore, we found no evidence of GPR18 coupling to $G\alpha_{15}$.

Potentiation of I_{GIRK} by NAGly but no GPR18-mediated potentiation of I_{GIRK}

Previous work has suggested GPR18 couples to $G\alpha_{i/o}$ protein signaling pathways (Kohno et al., 2006; McHugh et al., 2010; McHugh et al., 2012; Takenouchi et al., 2012), but we have not observed any GPR18-mediated inhibition of I_{Ca}, which is a primary downstream effector of $G\alpha_{i/o}$. We tested other effectors of $G\alpha_{i/o}$ proteins, including G protein-coupled inwardly-rectifying K+ currents (I_{GIRK}), to further investigate GPR18 signaling. GIRK channels expressed in SCG neurons open upon G protein activation by a $G\beta\gamma$-mediated mechanism.

SCG neurons do not endogenously express GIRK channels, so we injected cDNA encoding homomeric GIRK channel subunits, GIRK4 S143 (Vivaudou et al., 1997). I_{GIRK} was evoked at 0.1 Hz using a voltage ramp (Figure 9Ai, inset) in solutions designed to isolate I_{GIRK}. In SCG neurons expressing GIRK4 S143T, peak I_{GIRK} increased during NAGly treatment (Figure 9Ai and Aii). As a positive control for $G\alpha_{i/o}$ protein activation, NE was applied and peak I_{GIRK} also increased (Figure 9Ai and Aii). In SCG neurons expressing GIRK4 S143T and GPR18, both NAGly and NE potentiated I_{GIRK} (Figure 9Bi and Bii). NE significantly increased I_{GIRK} in SCG neurons expressing GIRK4 S143T with or without GPR18 (Figure 9C, one-way ANOVA, $p<0.001$). But the modulation of I_{GIRK} by NAGly was modest and only reached significance in SCG neurons expressing GIRK4

Molecular Pharmacology Fast Forward. Published on October 25, 2012 as DOI: 10.1124/mol.112.081182
This article has not been copyedited and formatted. The final version may differ from this version.

S143T alone with and without PTX treatment (Figure 9C), suggesting the effect of NAGly on I_{GIRK} is independent of GPR18 expression. Furthermore, NAGly's effect on I_{GIRK} is not $G\alpha_{i/o}$ protein-mediated since overnight PTX treatment did not block NAGly responses on I_{GIRK}, but did block NE responses (Figure 9C).

So NAGly activation of GPR18 was not observed with G protein modulation of I_{GIRK} currents as an assay.

No NAGly-induced change in cAMP levels in GPR18-expressing HEK cells

Another downstream effector of G proteins is adenylate cyclase, which converts adenosine triphosphate to cyclic adenosine monophosphate (cAMP). Live-cell cAMP levels were monitored in HEK cells transfected with the bioluminescence resonance energy transfer (BRET)-based cAMP sensor, CAMYEL (Jiang et al., 2007), loaded onto a multi-well luminescence plate reader. Net BRET was calculated from measurements of light intensity from the acceptor and donor channels following application of enzyme substrate, h-coelanterizene. High net BRET values indicate low intracellular cAMP levels and low net BRET values indicate high intracellular cAMP levels.

The ability of $G\alpha_{i/o}$ protein-coupled receptors to inhibit adenylate cyclase and reduce intracellular cAMP levels following forskolin stimulation was used as a measure of $G\alpha_{i/o}$ protein activation. Application of forskolin (1 μM) produced a decrease in net BRET and NAGly application failed to change net BRET levels in empty vector- or GPR18-expressing HEK cells (Figure 10Ai). A comparison of net BRET values 4 min after NAGly application shows no significant difference between empty vector and GPR18-expressing cells (Figure 10Aii, unpaired t-test, $p>0.05$). Samples preloaded with

Molecular Pharmacology Fast Forward. Published on October 25, 2012 as DOI: 10.1124/mol.112.081182
This article has not been copyedited and formatted. The final version may differ from this version.

NAGly 3 h before experiments did not significantly reduce the forskolin-induced decrease in net BRET (for empty vector, net BRET = 0.19 ± 0.004, n = 10; for GPR18-expressing HEKs, net BRET = 0.20 ± 0.005, n = 10; unpaired t-test, *p>0.05*). On the other hand, glutamate treatment of mGluR2-transfected HEK cells increased net BRET values following forskolin stimulation, which was blocked by overnight PTX treatment (Figure 10Bi). The increase in net BRET values 4 min after glutamate application was significant for the mGluR2-transfected group (Figure 10Bii, one-way ANOVA, *p<0.05*).

$G\alpha_s$-coupled pathways stimulate adenylate cyclase and the ability of GPCRs to increase intracellular cAMP levels was used as a measure of $G\alpha_s$-protein activation. NAGly did not significantly change net BRET levels in empty vector- or GPR18-expressing HEK cells (Figure 10C, unpaired t-test, *p>0.05*). But, dopamine applied to D_1R-transfected HEK cells was able to decrease net BRET values, which was blocked by overnight cholera toxin (CTX) treatment (Figure 10Di). Only the D_1R-transfected group significantly reduced net BRET values 4 min after dopamine application (Figure 10Dii, one-way ANOVA, *p<0.001*).

With the BRET-based cAMP sensor, we found no evidence of NAGly-mediated GPR18 coupling to $G\alpha_{i/o}$ or $G\alpha_s$ signaling pathways.

Molecular Pharmacology Fast Forward. Published on October 25, 2012 as DOI: 10.1124/mol.112.081182
This article has not been copyedited and formatted. The final version may differ from this version.

Discussion:

In the present study, we could not activate GPR18 that was heterologously expressed in a native neuronal system. NAGly is the proposed endogenous ligand for GPR18 (Kohno et al., 2006) and mediates microglia migration through a PTX-sensitive pathway (McHugh et al., 2010); however, we did not observe activation of $G\alpha_{i/o}$ protein signaling following NAGly application on heterologously expressed GPR18 in SCG neurons (Figure 3). Moreover, other putative agonists including anandamide, abnormal cannabidiol and O-1602 did not induce I_{Ca} inhibition in GPR18-injected SCG neurons (Figure 5). Likewise, a high-throughput screen of 43 lipid ligands, which included anandamide and NAGly, also failed to activate GPR18 (Yin et al., 2009). This was surprising because most, if not all, endogenous or heterologously expressed $G\alpha_{i/o}$ protein-coupled receptors in SCG neurons negatively-couple to N-type Ca^{2+} channels via a PTX-sensitive pathway. Instead, NAGly produced a consistent increase in I_{Ca} (Figure 3), similar to what has previously been reported by our lab (Guo et al., 2008a). As positive controls, NAGly potently inhibited heterologously expressed T-type Ca^{2+} channels confirming agonist activity (Figure 4), and full-length GPR18 protein was expressed and trafficked to the plasma membrane as demonstrated with the "rim-like" fluorescence pattern of a GFP-tagged version of the receptor (Figure 1) and positive staining of external HA-tagged GPR18 (Figure 2). However, in the absence of an actual receptor response, expression of functional GPR18 receptors in this study remains to be determined. A protein sequence alignment of GPR18 (Supplemental Figure 1C) suggests the mouse GPR18 clone used in our study is comparable to functional GPR18 in other studies (Kohno et al., 2006; McHugh et al., 2012; Qin et al., 2011) and capable of proper

Molecular Pharmacology Fast Forward. Published on October 25, 2012 as DOI: 10.1124/mol.112.081182
This article has not been copyedited and formatted. The final version may differ from this version.

protein expression. Other downstream effectors of $G\alpha_{i/o}$ were examined, but NAGly failed to activate GPR18. I_{GIRK} was potentiated by NAGly (Figure 9), but this effect was independent of GPR18 expression and $G\alpha_{i/o}$ protein coupling because 1) NAGly-induced potentiation of current was present in GIRK4 S143T alone injected SCG neurons and 2) augmentation of I_{GIRK} by NAGly persisted following overnight PTX treatment. In GPR18-expressing cells, cAMP levels were not altered by NAGly following forskolin-induced cAMP production (Figure 10A), suggesting no inhibition of adenylate cyclase by GPR18. Furthermore, GPR18 failed to couple to other $G\alpha$ proteins, $G\alpha_z$ (Figure 7) and $G\alpha_{15}$ (Figure 8), heterologously expressed in SCG neurons. We have previously demonstrated GPCR coupling to $G\alpha_z$ using agonist-mediated I_{Ca} inhibition (Jeong and Ikeda, 1998) but this is the first demonstration of negative coupling of activated $G\alpha_{15}$ to HVA-Ca^{2+} channels. Thus, modulation of N-type Ca^{2+} channels is a versatile assay of G protein activity since it is a common downstream effector of multiple G protein families.

Mutants of GPR18 that are predicted to confer constitutive activity, failed to tonically activate (i.e. in the absence of overt agonist) the receptor according to the measures of tonic G protein activity used in this study (Figure 6, Table 2). On the other hand, analogous mutations in ADRA2A (of the same class A of GPCRs as GPR18) were tonically active when expressed in rat sympathetic neurons (Figure 6B, Table 2). After expression of ADRA2A mutants, the basal FR, a sensitive indicator of tonic G protein activation (Ikeda, 1991), was significantly elevated (Table 2). This elevation was abolished after PTX treatment implicating tonic activation of endogenous $G\alpha_{i/o}$ proteins. It should be noted that some mutations designed to confer tonic activity of GPCRs also increase agonist potency (Cotecchia et al., 1990), suggesting tonic G protein activity may

Molecular Pharmacology Fast Forward. Published on October 25, 2012 as DOI: 10.1124/mol.112.081182
This article has not been copyedited and formatted. The final version may differ from this version.

actually represent increased sensitivity to endogenous agonist levels. This possibility cannot be excluded before testing receptor antagonists. Other possible consequences of tonic GPCR activity, such as activation of β-arrestin-mediated internalization, are not quantifiable with the electrophysiological techniques used in this study but may nevertheless occur. Redistribution of mutant GPR18 receptors into the ER of cells (Figure 6A) may reflect this mechanism, or mutations in the receptor may affect receptor trafficking. The lack of receptor expression at the plasma membrane may confound measurements of G protein activity. However, we have described other heterologously expressed GPCRs where GFP-fusion constructs are located primarily inside the cell but receptors maintain functional G protein signaling (Guo et al., 2008b). Thus, we infer that a small amount of GPCR expressed in the plasma membrane, which may not be noticeable with GFP-fusion constructs, is sufficient to carry out G protein activity. Assuming the mutations introduced into GPR18 were successful in producing a tonically active receptor, the inability to measure changes in basal G protein activity may indicate the existence of a mediator that couples GPR18 to G proteins, which is missing in SCG neurons or lost by cellular dialysis during whole-cell recordings. Heterodimerization of GPR18 with another GPCR may facilitate G protein signaling of GPR18 by heterodimer directed signaling (for reviews see Hudson et al., 2010; Marshall and Foord, 2010) and studies in endogenously expressing GPR18 cells may be necessary to find its GPCR binding partner and to recapitulate G protein signaling of GPR18.

The only positive responses of NAGly observed in this study were its direct effects on voltage-gated Ca^{2+} channels (Figure 3 and 4). Similar effects of lipoamino acids and arachidonic acid, a product of fatty acid amide hydrolase (FAAH) hydrolysis of

Molecular Pharmacology Fast Forward. Published on October 25, 2012 as DOI: 10.1124/mol.112.081182
This article has not been copyedited and formatted. The final version may differ from this version.

NAGly (Grazia Cascio et al., 2004), on ion channel function have been documented (Barbara et al., 2009; Chemin et al., 2007; Guo et al., 2008a). Although, it is unlikely the effects observed in this study are a result of NAGly breakdown to arachidonic acid and glycine because arachidonic acid reduces N-type Ca^{2+} channel amplitude (Liu and Rittenhouse, 2000) and the effect of NAGly on T-type Ca^{2+} channels is independent of FAAH activity (Barbara et al., 2009). NAGly has many reported actions: $G\alpha_{i/o}$-mediated activation of large-conductance Ca^{2+}-sensitive K^+ (BK) channels (Begg et al., 2003; Parmar and Ho, 2010), partial agonism of GPR92 (Oh et al., 2008), and blockade of glycine uptake via the glycine transporter, GLYT2 (Wiles et al., 2006), to name a few. Interestingly, NAGly is also a potent competitive substrate with anandamide for FAAH (Huang et al., 2001) and inhibiting FAAH can increase endogenous anandamide levels (Burstein et al., 2002). It is unclear which target of NAGly is responsible for the NAGly-induced cell migration or apoptosis observed in other recombinant systems (McHugh et al., 2010; McHugh et al., 2012; Takenouchi et al., 2012) or whether GPR18 signaling is cell-type dependent. For instance, if NAGly-induced signaling is intimately related to resting endocannabinoid levels, the lack of endogenous endocannabinoid production in SCG neurons (Won et al., 2009) may be responsible for this study's inability to reconstitute GPR18 signaling pathways.

GPR18-mediated signaling directly in neurons has not been demonstrated. GPR18 activity has been implicated in neuronal function by virtue of its regulation of microglial function (McHugh, 2012), but no detectable levels of GPR18 transcript are found in human brain (Gantz et al., 1997). The lack of receptors in neuronal tissues contradicts the abundance of endogenous NAGly in the spinal cord and brain (Huang et al., 2001) and

Molecular Pharmacology Fast Forward. Published on October 25, 2012 as DOI: 10.1124/mol.112.081182
This article has not been copyedited and formatted. The final version may differ from this version.

the ability of NAGly to affect neuronal activity. NAGly can modulate nociceptive signaling in the spinal cord (Huang et al., 2001; Vuong et al., 2008), though it is unclear if GPR18 signaling in microglia is responsible for this effect or if other targets of NAGly, such as GLYT2, play a more dominant role. NAGly can also indirectly affect neuronal excitability and synaptic transmission by altering circulating levels of endogenous endocannabinoids (Burstein et al., 2002), which can signal through CB_1Rs located throughout the CNS. The disconnect between localization of GPR18 and endogenous NAGly supports the presence of another receptor for NAGly, which is responsible for signaling in neurons. Other identified targets of NAGly may fulfill this role, but there remains a GPCR responsive to NAGly that can regulate neuronal activity. Two separate studies (Begg et al., 2003; Parmar and Ho, 2010) have implicated a NAGly-sensitive $G\alpha_{i/o}$-coupled receptor in the regulation of BK-channels, a channel that repolarizes the membrane potential and is an important regulator of action potential duration. This receptor has yet to be identified.

Conclusions

In a native neuronal system, heterologously expressed GPR18 is not activated by NAGly, thus corroborating the result obtained from the high-throughput screen of lipid ligands (Yin et al., 2009). This would argue against the de-orphanization of GPR18 until we have a better understanding of all of the elements involved in GPR18 signaling. Perhaps studies examining NAGly-mediated responses from endogenously expressing GPR18 cells will shed some light on this signaling pathway.

Authorship Contributions:

Participated in research design: Lu, Puhl, Ikeda

Conducted experiments: Lu

Contributed new reagents or analytic tools: Puhl

Performed data analysis: Lu

Wrote or contributed to writing of the manuscript: Lu, Puhl, Ikeda

References:

Barbara G, Alloui A, Nargeot J, Lory P, Eschalier A, Bourinet E and Chemin J (2009) T-type calcium channel inhibition underlies the analgesic effects of the endogenous lipoamino acids. *J Neurosci* **29**(42):13106-13114.

Begg M, Mo FM, Offertaler L, Batkai S, Pacher P, Razdan RK, Lovinger DM and Kunos G (2003) G protein-coupled endothelial receptor for atypical cannabinoid ligands modulates a Ca^{2+}-dependent K^+ current. *The Journal of biological chemistry* **278**(46):46188-46194.

Burstein SH, Huang SM, Petros TJ, Rossetti RG, Walker JM and Zurier RB (2002) Regulation of anandamide tissue levels by N-arachidonylglycine. *Biochem Pharmacol* **64**(7):1147-1150.

Burstein SH, McQuain CA, Ross AH, Salmonsen RA and Zurier RE (2011) Resolution of inflammation by N-arachidonoylglycine. *J Cell Biochem* **112**(11):3227-3233.

Chemin J, Nargeot J and Lory P (2007) Chemical determinants involved in anandamide-induced inhibition of T-type calcium channels. *The Journal of biological chemistry* **282**(4):2314-2323.

Cotecchia S, Exum S, Caron MG and Lefkowitz RJ (1990) Regions of the α_1-adrenergic receptor involved in coupling to phosphatidylinositol hydrolysis and enhanced sensitivity of biological function. *Proceedings of the National Academy of Sciences of the United States of America* **87**(8):2896-2900.

Elmslie KS, Zhou W and Jones SW (1990) LHRH and GTP-γ-S modify calcium current activation in bullfrog sympathetic neurons. *Neuron* **5**(1):75-80.

Gantz I, Muraoka A, Yang YK, Samuelson LC, Zimmerman EM, Cook H and Yamada T (1997) Cloning and chromosomal localization of a gene (GPR18) encoding a novel seven transmembrane receptor highly expressed in spleen and testis. *Genomics* **42**(3):462-466.

Giannone F, Malpeli G, Lisi V, Grasso S, Shukla P, Ramarli D, Sartoris S, Monsurro V, Krampera M, Amato E, Tridente G, Colombatti M, Parenti M and Innamorati G (2010) The puzzling uniqueness of the heterotrimeric G15 protein and its potential beyond hematopoiesis. *Journal of molecular endocrinology* **44**(5):259-269.

Gomeza J, Mary S, Brabet I, Parmentier ML, Restituito S, Bockaert J and Pin JP (1996) Coupling of metabotropic glutamate receptors 2 and 4 to $G\alpha_{15}$, $G\alpha_{16}$, and chimeric $G\alpha_{q/i}$ proteins: characterization of new antagonists. *Molecular pharmacology* **50**(4):923-930.

Grazia Cascio M, Minassi A, Ligresti A, Appendino G, Burstein S and Di Marzo V (2004) A structure-activity relationship study on N-arachidonoyl-amino acids as possible endogenous inhibitors of fatty acid amide hydrolase. *Biochem Biophys Res Commun* **314**(1):192-196.

Guo J and Ikeda SR (2004) Endocannabinoids modulate N-type calcium channels and G-protein-coupled inwardly rectifying potassium channels via CB_1 cannabinoid receptors heterologously expressed in mammalian neurons. *Molecular pharmacology* **65**(3):665-674.

Guo J and Ikeda SR (2005) Coupling of metabotropic glutamate receptor 8 to N-type Ca^{2+} channels in rat sympathetic neurons. *Molecular pharmacology* **67**(6):1840-1851.

Guo J, Williams DJ and Ikeda SR (2008a) N-arachidonoyl L-serine, a putative endocannabinoid, alters the activation of N-type Ca^{2+} channels in sympathetic neurons. *J Neurophysiol* **100**(2):1147-1151.

Guo J, Williams DJ, Puhl HL, 3rd and Ikeda SR (2008b) Inhibition of N-type calcium channels by activation of GPR35, an orphan receptor, heterologously expressed in rat sympathetic neurons. *J Pharmacol Exp Ther* **324**(1):342-351.

Hamill OP, Marty A, Neher E, Sakmann B and Sigworth FJ (1981) Improved patch-clamp techniques for high-resolution current recording from cells and cell-free membrane patches. *Pflugers Arch* **391**(2):85-100.

Herlitze S, Garcia DE, Mackie K, Hille B, Scheuer T and Catterall WA (1996) Modulation of Ca^{2+} channels by G-protein βγ subunits. *Nature* **380**(6571):258-262.

Huang SM, Bisogno T, Petros TJ, Chang SY, Zavitsanos PA, Zipkin RE, Sivakumar R, Coop A, Maeda DY, De Petrocellis L, Burstein S, Di Marzo V and Walker JM (2001) Identification of a new class of molecules, the arachidonyl amino acids, and characterization of one member that inhibits pain. *The Journal of biological chemistry* **276**(46):42639-42644.

Hudson BD, Hebert TE and Kelly ME (2010) Ligand- and heterodimer-directed signaling of the CB_1 cannabinoid receptor. *Molecular pharmacology* **77**(1):1-9.

Ikeda SR (1991) Double-pulse calcium channel current facilitation in adult rat sympathetic neurones. *The Journal of physiology* **439**:181-214.

Ikeda SR (1992) Prostaglandin modulation of Ca^{2+} channels in rat sympathetic neurones is mediated by guanine nucleotide binding proteins. *The Journal of physiology* **458**:339-359.

Ikeda SR (1996) Voltage-dependent modulation of N-type calcium channels by G-protein βγ subunits. *Nature* **380**(6571):255-258.

Ikeda SR (2004) Expression of G-protein signaling components in adult mammalian neurons by microinjection. *Methods Mol Biol* **259**:167-181.

Ikeda SR and Jeong SW (2004) Use of RGS-insensitive Gα subunits to study endogenous RGS protein action on G-protein modulation of N-type calcium channels in sympathetic neurons. *Methods Enzymol* **389**:170-189.

Ikeda SR, Lovinger DM, McCool BA and Lewis DL (1995) Heterologous expression of metabotropic glutamate receptors in adult rat sympathetic neurons: subtype-specific coupling to ion channels. *Neuron* **14**(5):1029-1038.

Ikeda SR, Schofield GG and Weight FF (1987) Somatostatin blocks a calcium current in acutely isolated adult rat superior cervical ganglion neurons. *Neurosci Lett* **81**(1-2):123-128.

Jacoby E (2006) Designing compound libraries targeting GPCRs. *Ernst Schering Found Symp Proc*(2):93-103.

Jarai Z, Wagner JA, Varga K, Lake KD, Compton DR, Martin BR, Zimmer AM, Bonner TI, Buckley NE, Mezey E, Razdan RK, Zimmer A and Kunos G (1999) Cannabinoid-induced mesenteric vasodilation through an endothelial site distinct

from CB_1 or CB_2 receptors. *Proceedings of the National Academy of Sciences of the United States of America* **96**(24):14136-14141.

Jeong SW and Ikeda SR (1998) G protein α subunit $G\alpha_z$ couples neurotransmitter receptors to ion channels in sympathetic neurons. *Neuron* **21**(5):1201-1212.

Jiang LI, Collins J, Davis R, Lin KM, DeCamp D, Roach T, Hsueh R, Rebres RA, Ross EM, Taussig R, Fraser I and Sternweis PC (2007) Use of a cAMP BRET sensor to characterize a novel regulation of cAMP by the sphingosine 1-phosphate/G13 pathway. *The Journal of biological chemistry* **282**(14):10576-10584.

Kammermeier PJ, Ruiz-Velasco V and Ikeda SR (2000) A voltage-independent calcium current inhibitory pathway activated by muscarinic agonists in rat sympathetic neurons requires both $G\alpha_{q/11}$ and Gβγ. *J Neurosci* **20**(15):5623-5629.

Kjelsberg MA, Cotecchia S, Ostrowski J, Caron MG and Lefkowitz RJ (1992) Constitutive activation of the α_{1B}-adrenergic receptor by all amino acid substitutions at a single site. Evidence for a region which constrains receptor activation. *The Journal of biological chemistry* **267**(3):1430-1433.

Kohno M, Hasegawa H, Inoue A, Muraoka M, Miyazaki T, Oka K and Yasukawa M (2006) Identification of N-arachidonylglycine as the endogenous ligand for orphan G-protein-coupled receptor GPR18. *Biochem Biophys Res Commun* **347**(3):827-832.

Laemmli UK (1970) Cleavage of structural proteins during the assembly of the head of bacteriophage T4. *Nature* **227**(5259):680-685.

Liu L and Rittenhouse AR (2000) Effects of arachidonic acid on unitary calcium currents in rat sympathetic neurons. *The Journal of physiology* **525 Pt 2**:391-404.

Lu VB, Williams DJ, Won YJ and Ikeda SR (2009) Intranuclear microinjection of DNA into dissociated adult mammalian neurons. *J Vis Exp*(34).

Marshall FH and Foord SM (2010) Heterodimerization of the $GABA_B$ receptor-implications for GPCR signaling and drug discovery. *Adv Pharmacol* **58**:63-91.

McHugh D (2012) GPR18 in Microglia: implications for the CNS and endocannabinoid system signalling. *Br J Pharmacol*.

McHugh D, Hu SS, Rimmerman N, Juknat A, Vogel Z, Walker JM and Bradshaw HB (2010) N-arachidonoyl glycine, an abundant endogenous lipid, potently drives directed cellular migration through GPR18, the putative abnormal cannabidiol receptor. *BMC Neurosci* **11**:44.

McHugh D, Page J, Dunn E and Bradshaw HB (2012) Δ(9) -Tetrahydrocannabinol and N-arachidonyl glycine are full agonists at GPR18 receptors and induce migration in human endometrial HEC-1B cells. *Br J Pharmacol* **165**(8):2414-2424.

Oh DY, Yoon JM, Moon MJ, Hwang JI, Choe H, Lee JY, Kim JI, Kim S, Rhim H, O'Dell DK, Walker JM, Na HS, Lee MG, Kwon HB, Kim K and Seong JY (2008) Identification of farnesyl pyrophosphate and N-arachidonylglycine as endogenous ligands for GPR92. *The Journal of biological chemistry* **283**(30):21054-21064.

Parmar N and Ho WS (2010) N-arachidonoyl glycine, an endogenous lipid that acts as a vasorelaxant via nitric oxide and large conductance calcium-activated potassium channels. *Br J Pharmacol* **160**(3):594-603.

Qin Y, Verdegaal EM, Siderius M, Bebelman JP, Smit MJ, Leurs R, Willemze R, Tensen CP and Osanto S (2011) Quantitative expression profiling of G-protein-coupled

receptors (GPCRs) in metastatic melanoma: the constitutively active orphan GPCR GPR18 as novel drug target. *Pigment Cell Melanoma Res* **24**(1):207-218.

Ren Q, Kurose H, Lefkowitz RJ and Cotecchia S (1993) Constitutively active mutants of the α_2-adrenergic receptor. *The Journal of biological chemistry* **268**(22):16483-16487.

Scheer A, Fanelli F, Costa T, De Benedetti PG and Cotecchia S (1996) Constitutively active mutants of the α_{1B}-adrenergic receptor: role of highly conserved polar amino acids in receptor activation. *EMBO J* **15**(14):3566-3578.

Scheer A, Fanelli F, Costa T, De Benedetti PG and Cotecchia S (1997) The activation process of the α_{1B}-adrenergic receptor: potential role of protonation and hydrophobicity of a highly conserved aspartate. *Proceedings of the National Academy of Sciences of the United States of America* **94**(3):808-813.

Takenouchi R, Inoue K, Kambe Y and Miyata A (2012) N-arachidonoyl glycine induces macrophage apoptosis via GPR18. *Biochem Biophys Res Commun* **418**(2):366-371.

Vivaudou M, Chan KW, Sui JL, Jan LY, Reuveny E and Logothetis DE (1997) Probing the G-protein regulation of GIRK1 and GIRK4, the two subunits of the KACh channel, using functional homomeric mutants. *The Journal of biological chemistry* **272**(50):31553-31560.

Vuong LA, Mitchell VA and Vaughan CW (2008) Actions of N-arachidonyl-glycine in a rat neuropathic pain model. *Neuropharmacology* **54**(1):189-193.

Wiles AL, Pearlman RJ, Rosvall M, Aubrey KR and Vandenberg RJ (2006) N-Arachidonyl-glycine inhibits the glycine transporter, GLYT2a. *J Neurochem* **99**(3):781-786.

Williams DJ, Puhl HL and Ikeda SR (2010) A Simple, Highly Efficient Method for Heterologous Expression in Mammalian Primary Neurons Using Cationic Lipid-mediated mRNA Transfection. *Front Neurosci* **4**:181.

Won YJ, Puhl HL, 3rd and Ikeda SR (2009) Molecular reconstruction of mGluR5a-mediated endocannabinoid signaling cascade in single rat sympathetic neurons. *J Neurosci* **29**(43):13603-13612.

Yin H, Chu A, Li W, Wang B, Shelton F, Otero F, Nguyen DG, Caldwell JS and Chen YA (2009) Lipid G protein-coupled receptor ligand identification using β-arrestin PathHunter assay. *The Journal of biological chemistry* **284**(18):12328-12338.

Zhu Y and Ikeda SR (1993) Adenosine modulates voltage-gated Ca^{2+} channels in adult rat sympathetic neurons. *J Neurophysiol* **70**(2):610-620.

Zhu Y and Ikeda SR (1994) VIP inhibits N-type Ca^{2+} channels of sympathetic neurons via a pertussis toxin-insensitive but cholera toxin-sensitive pathway. *Neuron* **13**(3):657-669.

Molecular Pharmacology Fast Forward. Published on October 25, 2012 as DOI: 10.1124/mol.112.081182
This article has not been copyedited and formatted. The final version may differ from this version.

Footnotes:

a) Financial support

This research was supported by the Intramural Research Program of the National Institutes of Health [National Institute on Alcohol Abuse and Alcoholism].

b) Previously presented

V.B. Lu, H.L. Puhl III and S.R. Ikeda. N-arachidonyl glycine (NAGly) does not activate heterologously expressed G-protein receptor 18 (GPR18) in a native neuronal system. Program No. 38.12. *2011 Neuroscience Meeting Planner*. Washington, DC: Society for Neuroscience, 2011. Online.

c) Send reprint requests to

Stephen R. Ikeda

5625 Fishers Lane, Room TS-11, MSC 9411

Bethesda, MD, 20892, USA (regular mail)

Email: sikeda@mail.nih.gov

Molecular Pharmacology Fast Forward. Published on October 25, 2012 as DOI: 10.1124/mol.112.081182
This article has not been copyedited and formatted. The final version may differ from this version.

Figure Legends:

Figure 1: Expression and localization of heterologously expressed GPR18-EGFP. Confocal images of A) GPR18-EGFP, B) EGFP, and C) EGFP-KRas tail constructs expressed in SCG neurons (top panels) or HeLa cells (bottom panels). Insets of top panels: line plots of fluorescence intensity from dashed line across injected SCG neuron. Note the "rim-like" fluorescence of the GPR18-EGFP construct, similar to the membrane-bound EGFP-KRas tail-expressing cells and different from cytosolic EGFP-expressing cells. Scale bar is 20 μm. D) Sample Western blot of EGFP-tagged constructs. Primary anti-GFP antibody (1:2000, NeuroMab) and secondary anti-mouse HRP-conjugated antibody (1:1000, Thermo) were used. Band in GPR18-EGFP lane at approximately 80 kD, band in EGFP lane at 27 kD and band in EGFP-KRas tail lane at 29 kD. E) Stripped and reprobed blot for loading controls α-tubulin (1:2000, Cell Signaling) and cyclophilin B (1:5000, Abcam) corresponding to bands at 51 and 19 kD, respectively.

Figure 2: Live-cell staining and imaging of HA-tagged GPR18. Confocal images of stained HeLa cells transfected with A) 3xHA-GPR18 or external HA-tagged GPR18, B and C) GPR18-3xHA or internal HA-tagged GPR18. EGFP was co-transfected to label transfected cells. A and B) Live-cell staining with biotin-labeled anti-HA antibody (1:200, Covance) and streptavidin conjugated Qdot®655 secondary antibody (1:200, Molecular Probes). C) HA-staining followed fixation and permeabilization of HeLa cells. First panels are images obtained from the GFP channel (500-550 nm emission band-pass filter),

Molecular Pharmacology Fast Forward. Published on October 25, 2012 as DOI: 10.1124/mol.112.081182
This article has not been copyedited and formatted. The final version may differ from this version.

second panels are fluorescent images from the far-red channel (650-710 nm emission band-pass filter), and the last panels are merged images pseudo-colored green and purple. Scale bar is 20 μm.

Figure 3: NAGly-mediated potentiation of N-type ($Ca_v2.2$) Ca^{2+} channel currents (I_{Ca}) in rat SCG neurons. Data are from whole cell patch-clamp recordings of rat sympathetic neurons obtained at room temperature (20-24°C). Ai) Sample superimposed I_{Ca} traces evoked from an uninjected SCG neuron using the double-pulse I_{Ca} protocol, shown as inset. Two 25 ms test pulses to +10 mV from a holding potential of -80 mV, separated by a 50 ms conditioning pulse to +80 mV. For both sample traces displayed in Figure, solid black trace is the baseline I_{Ca}, solid grey trace is the I_{Ca} during application of 10 μM N-arachidonyl glycine (NAGly), Y-axis scale bar is 0.5 nA and X-axis scale bar is 10 ms. Aii) Time course of I_{Ca} amplitude in an uninjected neuron during exposure to 1 and 10 μM NAGly (solid grey line) and 10 μM norepinephrine (NE, dashed black line). ○ represents the prepulse I_{Ca}, ● represents the postpulse I_{Ca}. Aiii) Time course of the facilitation ratio (FR) of the same sample cell in Aii during exposure to 1 and 10 μM NAGly and 10 μM NE. B) Ca^{2+} current-voltage relationship of uninjected neuron before (○) and during 10 μM NAGly (●) application. Note the voltage-dependent enhancement of Ca^{2+} currents and the hyperpolarizing shift in the IV curve peak. Ci) Sample superimposed I_{Ca} traces evoked from an untagged GPR18-injected SCG neuron using the double-pulse protocol. Cii) Time course of I_{Ca} amplitude in an untagged GPR18-injected neuron during exposure to 1 and 10 μM NAGly (solid grey line) and 10 μM norepinephrine (NE, dashed black line). Ciii) Time course of the FR of the same sample

Molecular Pharmacology Fast Forward. Published on October 25, 2012 as DOI: 10.1124/mol.112.081182
This article has not been copyedited and formatted. The final version may differ from this version.

cell in Cii during exposure to 1 and 10 μM NAGly and 10 μM NE. D) Changes in I_{Ca} amplitude produced by NAGly (1 or 10 μM) and NE (10 μM) from each cell are represented as individual points in the dot plot graph. Drug responses were normalized to baseline I_{Ca} using the equation $I_{drug}/I_{baseline}$ x 100, where I_{drug} and $I_{baseline}$ are I_{Ca} amplitudes during and before drug application, respectively. Mean ± SEM drug responses represented as lines on graph. N's for each group are indicated on graph in brackets. Means values between uninjected and untagged GPR18-injected neurons were not significantly different (unpaired t-test, *p>0.05*).

Figure 4: NAGly-mediated inhibition of LVA-I_{Ca} heterologously expressed in rat SCG neurons. A) Sample I_{Ca} trace from an uninjected SCG neuron, elicited by the low-voltage I_{Ca} protocol illustrated as inset. Two 25 ms test pulses, the first to -40 mV and the second to +10 mV, separated by a 60 ms pulse to -60 mV to inactivate LVA-I_{Ca}. B) Sample superimposed I_{Ca} traces from a $Ca_v3.1$-injected SCG neuron, elicited by the low-voltage I_{Ca} protocol. For all sample traces displayed in Figure, solid black trace is the baseline I_{Ca}, solid grey trace is the I_{Ca} during application of 10 μM NAGly, Y-axis scale bar is 0.5 nA and X-axis scale bar is 10 ms. Note the inhibition of LVA-I_{Ca} elicited during the first test pulse and the potentiation of HVA-I_{Ca} elicited during the second test pulse by application of NAGly. C) Sample superimposed I_{Ca} traces from an SCG neuron co-injected with $Ca_v3.1$ and GPR18, elicited by the low-voltage I_{Ca} protocol. In this set of experiments, an untagged version of GPR18 was used. D) Changes in I_{Ca} amplitude, both LVA- and HVA-I_{Ca}, produced by NAGly (10 μM) from each cell are represented as individual points in the dot plot graph. NAGly responses were normalized to baseline I_{Ca}. Mean ±

Molecular Pharmacology Fast Forward. Published on October 25, 2012 as DOI: 10.1124/mol.112.081182
This article has not been copyedited and formatted. The final version may differ from this version.

SEM NAGly responses represented as lines on graph. N's for each group are indicated on graph in brackets. Mean values between $Ca_v3.1$ alone and $Ca_v3.1$ with GPR18-injected groups were not significantly different (unpaired t-test, *p>0.05*).

Figure 5: Effectiveness of various proposed agonists of GPR18 to inhibit I_{Ca} in GPR18- or CB_1R-expressing SCG neurons. In this set of experiments, an untagged version of GPR18 was used. N-arachidonoyl-L-serine (ARA-S), anandamide (AEA) and norepinephrine (NE) were applied to uninjected, GPR18- and CB_1R-injected neurons. Due to lack of a confirmed endogenous receptor, abnormal cannabidiol (Abn-Cbd) and O-1602 were applied to uninjected and GPR18-injected neurons only. Changes in I_{Ca} amplitude in response to various agonists from each cell are represented as individual points in the dot plot graph, normalized to baseline I_{Ca}. Mean ± SEM drug responses represented as lines on graph. N's for each group are indicated on graph in brackets. For ARA-S, AEA and NE treatment groups, a one-way ANOVA followed by Newman-Keuls post-test was used to compare groups. For Abn-Cbd and O-1602, an unpaired t-test was used. * = *p<0.05*, *** = *p<0.001*.

Figure 6: Mutant class A GPCRs designed to induce or alter tonic activity of receptors. A) Left: Confocal image of GPR18 D118T-EGFP construct expressed in HeLa cells. Note the fluorescence primarily inside of the cell in the internal membrane network, reminiscent of the endoplasmic reticulum. Scale bar is 20 µm. Right: Sample superimposed I_{Ca} traces from an untagged GPR18 D118T-injected SCG neuron, elicited by the double-pulse I_{Ca} protocol. For all sample traces displayed in Figure, solid black

Molecular Pharmacology Fast Forward. Published on October 25, 2012 as DOI: 10.1124/mol.112.081182
This article has not been copyedited and formatted. The final version may differ from this version.

trace is the baseline I_{Ca}, dashed black trace is the I_{Ca} during application of 10 μM NE, solid grey trace is the I_{Ca} during application of 10 μM NAGly, Y-axis scale bar is 0.5 nA and X-axis scale bar is 10 ms. Horizontal dashed grey line from the peak of the postpulse I_{Ca} highlights the relief of tonic Ca^{2+} channel inhibition by the conditioning pulse. B) Sample superimposed I_{Ca} traces from an ADRA2A D130T-injected SCG neuron, elicited by the double-pulse I_{Ca} protocol. Note the kinetic slowing and inhibition of prepulse I_{Ca} and the large relief of tonic Ca^{2+} channel inhibition by the conditioning pulse in the baseline I_{Ca} trace. C) Responses of a proposed non-constitutively active mutant of GPR18, GPR18 A108N (Qin et al., 2011), to NAGly and other agonists of GPR18. Left: Confocal image of GPR18 A108N-EGFP construct expressed in HeLa cells. Note the "rim-like" fluorescence in transfected cells. Scale bar is 20 μm. Right: Sample superimposed I_{Ca} traces from an untagged GPR18 A108N-injected SCG neuron, elicited by the double-pulse I_{Ca} protocol. Below: Time course of I_{Ca} amplitude in an untagged GPR18 A108N-expressing neuron during exposure to 10 μM NAGly, 10 μM AEA and 10 μM Abn-Cbd. ○ represents the prepulse I_{Ca}, ● represents the postpulse I_{Ca}. Note the potentiation of pre- and postpulse I_{Ca} following application of NAGly, and lack of I_{Ca} response to AEA and Abn-Cbd application. D) Changes in I_{Ca} amplitude, normalized to baseline I_{Ca}, from each cell are represented as individual points in the dot plot graph. Mean ± SEM drug responses represented as lines on graph. N's for each group are indicated on graph in brackets. To compare groups, a one-way ANOVA followed by Newman-Keuls post-test was used. * = $p<0.05$, *** = $p<0.001$.

Molecular Pharmacology Fast Forward. Published on October 25, 2012 as DOI: 10.1124/mol.112.081182
This article has not been copyedited and formatted. The final version may differ from this version.

Figure 7: Functional coupling of endogenous α_2-adrenergic receptors to $G\alpha_z$ but not untagged GPR18. Ai) Sample superimposed I_{Ca} traces evoked from a $G\alpha_z$-injected SCG neuron using the double-pulse I_{Ca} protocol. For both sample traces displayed in Figure, solid black trace is the baseline I_{Ca}, dashed black trace is the I_{Ca} during application of 10 μM NE, solid grey trace is the I_{Ca} during application of 10 μM NAGly, Y-axis scale bar is 0.5 nA and X-axis scale bar is 10 ms. Aii) Time course of I_{Ca} amplitude in a $G\alpha_z$-injected neuron during exposure to 10 μM NAGly (solid grey line) and 10 μM NE (dashed black line). ○ represents the prepulse I_{Ca}, ● represents the postpulse I_{Ca}. Note the slower onset and off-rate of NE compared to uninjected SCG neurons (Figure 3Aii). Aiii) Time course of the facilitation ratio (FR) of the same sample cell in Aii during exposure to 10 μM NAGly and 10 μM NE. Bi) Sample superimposed I_{Ca} traces evoked from an SCG neuron co-expressing $G\alpha_z$ and untagged GPR18, using the double-pulse I_{Ca} protocol. Bii) Time course of I_{Ca} amplitude in a $G\alpha_z$ + untagged GPR18-injected neuron during exposure to 10 μM NAGly (solid grey line) and 10 μM NE (dashed black line). Biii) Time course of FR of the same sample cell as in Bii. C) Changes in I_{Ca} amplitude produced by NAGly (10 μM) and NE (10 μM) from each cell are represented as individual points in the dot plot graph. Mean ± SEM drug responses represented as lines on graph. NE-mediated responses were elicited from SCG neurons following overnight PTX treatment. N's for each group are indicated on graph in brackets. To compare groups, a one-way ANOVA followed by Newman-Keuls post-test was performed. *** = $p<0.001$. D) Testing possible coupling of constitutively active GPR18 with $G\alpha_z$ in SCG neurons. Di) The basal FR, a sensitive indicator of tonic receptor activity, was determined from the ratio of postpulse to prepulse I_{Ca} of the first recording obtained from each cell. Basal FR

Molecular Pharmacology Fast Forward. Published on October 25, 2012 as DOI: 10.1124/mol.112.081182
This article has not been copyedited and formatted. The final version may differ from this version.

values from each cell are represented as individual points in the dot plot graph. Mean ± SEM basal FR represented as lines on graph. To compare groups, a one-way ANOVA followed by Newman-Keuls post-test was performed. *** = $p<0.001$. Dii) Changes in I_{Ca} amplitude in response to NE, normalized to baseline I_{Ca}, from each cell are represented as individual points in the dot plot graph. Mean ± SEM NE response represented as lines on graph. No significant difference was observed between groups, as determined by one-way ANOVA followed by Newman-Keuls post-test ($p>0.05$).

Figure 8: Functional coupling of heterologously expressed mGluR2 receptors to $G\alpha_{15}$ but not untagged GPR18. A) Demonstration of functional coupling of mGluR2 to $G\alpha_{15}$. For controls of functional coupling to $G\alpha_{15}$, see Supplementary Figure 3. Ai) Sample superimposed I_{Ca} traces evoked from an SCG neuron co-expressing $G\alpha_{15}\beta_1\gamma_2$ and mGluR2 using the double-pulse I_{Ca} protocol, following overnight PTX treatment. For both sample traces displayed in Figure, solid black trace is the baseline I_{Ca}, dashed black trace is the I_{Ca} during application of 10 μM NE, dashed grey trace is the I_{Ca} during application of 100 μM glutamate, Y-axis scale bar is 0.5 nA and X-axis scale bar is 10 ms. Aii) Time course of I_{Ca} amplitude in a $G\alpha_{15}\beta_1\gamma_2$ + mGluR2-injected neuron during exposure to 10 μM NE (dashed black line) and 100 μM glutamate (dashed grey line). ○ represents the prepulse I_{Ca}, ● represents the postpulse I_{Ca}. Aiii) Time course of the facilitation ratio (FR) of the same sample cell in Aii during exposure to 10 μM NE and 100 μM glutamate. Bi) Sample superimposed I_{Ca} traces evoked from an SCG neuron co-expressing $G\alpha_{15}\beta_1\gamma_2$ and untagged GPR18, using the double-pulse I_{Ca} protocol, following overnight PTX treatment. Bii) Time course of I_{Ca} amplitude in an SCG neuron co-

Molecular Pharmacology Fast Forward. Published on October 25, 2012 as DOI: 10.1124/mol.112.081182
This article has not been copyedited and formatted. The final version may differ from this version.

expressing $G\alpha_{15}\beta_1\gamma_2$ and untagged GPR18 during exposure to 10 μM NAGly (solid grey line) and 10 μM NE (dashed black line). Biii) Time course of the FR of the same sample cell in Bii. C) Changes in I_{Ca} amplitude produced by NAGly (10 μM) and NE (10 μM) from each cell are represented as individual points in the dot plot graph. Mean ± SEM drug response represented as lines on graph. Drug responses were tested in SCG neurons following overnight PTX treatment. N's for each group are indicated on graph in brackets. To compare groups, a one-way ANOVA followed by Newman-Keuls post-test was performed, but no significant difference was observed ($p>0.05$). D) To test possible coupling of constitutively active GPR18 with $G\alpha_{15}$ in SCG neurons, basal I_{Ca} density was measured. Basal I_{Ca} density was determined from the postpulse I_{Ca} divided by the capacitance of the cell, calculated from integrating the area under the current trace obtained from a +10 mV step applied before cell capacitance compensation. I_{Ca} density values from each cell are represented as individual points in the dot plot graph. Mean ± SEM I_{Ca} density represented as lines on graph. I_{Ca} density was measured in SCG neurons following overnight PTX treatment. To compare groups, a one-way ANOVA followed by Newman-Keuls post-test was performed. * = $p<0.05$.

Figure 9: Testing modulation of G protein-coupled inwardly-rectifying K^+ (GIRK) channels by untagged GPR18. Ai) Sample superimposed I_{GIRK} traces evoked from a GIRK4 S143T-injected SCG neuron using the voltage ramp, shown as inset. A 200 ms voltage ramp from -140 to -40 mV, from a holding potential of -60 mV, was used to elicit I_{GIRK}. For both sample traces displayed in Figure, solid black trace is the baseline I_{GIRK}, dashed black trace is the I_{GIRK} during application of 10 μM NE, solid grey trace is the

Molecular Pharmacology Fast Forward. Published on October 25, 2012 as DOI: 10.1124/mol.112.081182
This article has not been copyedited and formatted. The final version may differ from this version.

I_{GIRK} during application of 10 μM NAGly and Y-axis scale bar is 1 nA. Aii) Time course of I_{GIRK} amplitude in a GIRK4 S143T-injected neuron during exposure to 10 μM NAGly (solid grey line) and 10 μM NE (dashed black line). Bi) Sample superimposed I_{GIRK} traces evoked from an SCG neuron co-injected with GIRK4 S143T and untagged GPR18 using the I_{GIRK} voltage ramp protocol. Bii) Time course of I_{GIRK} amplitude in a GIRK4 S143T + GPR18-injected neuron during exposure to 10 μM NAGly (solid grey line) and 10 μM NE (dashed black line). C) Changes in I_{GIRK} amplitude produced by NAGly (10 μM) and NE (10 μM) from each cell are represented as individual points in the dot plot graph. Drug responses were normalized to baseline I_{GIRK}. Mean ± SEM drug responses represented as lines on graph. N's for each group are indicated on graph in brackets. To compare groups, a one-way ANOVA followed by Newman-Keuls post-test was performed. * = $p<0.05$, *** = $p<0.001$.

Figure 10: Monitoring modulation of adenylate cyclase using the BRET-based cAMP sensor CAMYEL. Data are obtained from live HEK cells loaded in a microplate luminometer. HEK cells were transfected with empty vector or selected G protein-coupled receptor cDNA, CAMYEL cDNA and PEI. Approximately 16 h post-transfection, cells were transferred to a black 96-well microplate and loaded into a luminometer for recording. Net BRET was calculated as $A/D - d$, where A is the light intensity measured from the acceptor channel (542/27 nm) for 1 s, D is the light intensity measured from the donor channel (460/60 nm) for 1 s, and d is the background or spectral overlap, calculated previously as the A/D value for Rluc8 alone. Net BRET values are inversely related to cAMP levels (high net BRET = low intracellular cAMP levels, low

Molecular Pharmacology Fast Forward. Published on October 25, 2012 as DOI: 10.1124/mol.112.081182
This article has not been copyedited and formatted. The final version may differ from this version.

net BRET = high intracellular cAMP levels). A and B) Test of $G\alpha_{i/o}$-mediated inhibition of forskolin stimulated cAMP production. Ai) Time course of net BRET readings from empty vector and untagged GPR18-expressing HEK cells. Legend: F = forskolin (1 μM), NG = NAGly (10 μM). Aii) Net BRET values 4 min after injection of NAGly from each sample well are represented as individual points in the dot plot graph. Mean ± SEM net BRET values are represented as lines on graph. N's for each group are indicated on graph in brackets. No significant difference was observed between empty vector and GPR18-transfected cells (unpaired t-test, *p>0.05*). Bi) Time course of net BRET readings from empty vector and mGluR2-expressing HEK cells. Legend: F = forskolin (1 μM), G = glutamate (100 μM). Pertussis toxin (PTX) was applied to HEK cells during overnight incubation. Bii) Net BRET values 4 min after injection of glutamate from each sample well are represented as individual points in the dot plot graph. Mean ± SEM net BRET values are represented as lines on graph. A significant increase in mean net BRET value following glutamate application was observed in the mGluR2-transfected group (one-way ANOVA followed by Newman-Keuls post-test, *** = *p<0.001*). C and D) Test of $G\alpha_s$-mediated stimulation of cAMP production. Ci) Time course of net BRET readings from empty vector and untagged GPR18-expressing HEK cells. Legend: NG = NAGly (10 μM), F = forskolin (10 μM). Cii) Net BRET values 4 min after injection of NAGly from each sample well are represented as individual points in the dot plot graph. Mean ± SEM net BRET values are represented as lines on graph. No significant difference was observed between empty vector and GPR18-transfected cells (unpaired t-test, *p>0.05*). Di) Time course of net BRET readings from empty vector and D_1R-expressing HEK cells. Legend: D = dopamine hydrochloride (10 μM), F = forskolin (10 μM). Cholera toxin

(CTX) was applied to HEK cells during overnight incubation. Dii) Net BRET values 4 min after injection of dopamine from each sample well are represented as individual points in the dot plot graph. Mean ± SEM net BRET values are represented as lines on graph. A significant decrease in mean net BRET value following dopamine application was observed in the D_1R-transfected group (one-way ANOVA followed by Newman-Keuls post-test, *** = $p<0.001$).

Molecular Pharmacology Fast Forward. Published on October 25, 2012 as DOI: 10.1124/mol.112.081182
This article has not been copyedited and formatted. The final version may differ from this version.

Table 1: Primers for QuikChange™ site-directed mutagenesis. Point mutations of GPR18 and ADRA2A were generated using a QuikChange™ site-directed mutagenesis strategy and the primer sets listed in table, which were commercially synthesized (IDT). All mutant constructs were confirmed by DNA sequencing.

Point mutation	*Forward primer (5' to 3' end)*	*Reverse primer (5' to 3' end)*
GPR18 A108N	GGTGGTGTTTTACCCAAGCCTCAATC TGTGGCTTCTTGC	GCAAGAAGCCACAGATTGAGGCTTGG GTAAAACACCACC
GPR18 N40A	GGGCTGTTTGTTGCTGTCACTGCGTT GTGGG	CCCACAACGCAGTGACAGCAACAAAC AGCCC
GPR18 D118A	GCTTTCATTAGTGCTGCCAGATACAT GGCCATCG	CGATGGCCATGTATCTGGCAGCACTA ATGAAAGC
GPR18 D118T	GCTTTCATTAGTGCTACCAGATACAT GGCCATCG	CGATGGCCATGTATCTGGTAGCACTA ATGAAAGC
GPR18 I231E	GGTCAAGGAGAAGTCCGAACGGATCA TCATGACC	GGTCATGATGATCCGTTCGGACTTCT CCTTGACC
ADRA2A N51A	CCGTGTTCGGCGCCGTGCTTGTCATC ATTGCCG	CGGCAATGATGACAAGCACGGCGCCG AACACGG
ADRA2A D130A	CCATCAGCTTGGCTCGTTACTGGTCC	GGACCAGTAACGAGCCAAGCTGATGG
ADRA2A D130T	CCATCAGCTTGACTCGTTACTGGTCC	GGACCAGTAACGAGTCAAGCTGATGG
ADRA2A T373E	CCGCGAGAAGCGCTTCGAATTCGTGC TGGCGG	CCGCCAGCACGAATTCGAAGCGCTTC TCGCGG

Molecular Pharmacology Fast Forward. Published on October 25, 2012 as DOI: 10.1124/mol.112.081182
This article has not been copyedited and formatted. The final version may differ from this version.

Table 2: Summary of constitutively active mutants (CAMs). Mutants and ADRA2A alone were injected into SCG neurons and Ca^{2+} currents (I_{Ca}) were elicited using the double-pulse protocol. Basal facilitation ratio (FR), a sensitive indicator of tonic receptor activity, was determined from the ratio of postpulse to prepulse I_{Ca} of the first recording obtained from each cell. NE-responses were normalized to baseline I_{Ca} using the equation $I_{drug}/I_{baseline}$ x 100, where I_{drug} and $I_{baseline}$ are Ca^{2+} current amplitudes during and before NE application, respectively. The I_{Ca} density was determined from the postpulse I_{Ca} divided by the capacitance of the cell, calculated from integrating the area under the current trace obtained from a +10 mV step applied before cell capacitance compensation. Mean ± SEM values are indicated with number of cells in brackets. Unpaired t-tests were performed to compare each untagged GPR18 mutant with the analogous ADRA2A mutant. To account for multiple comparisons, a Bonferroni correction was used and a *p-value < 0.017* (#) was taken as statistically significant.

Construct	*Basal FR*	*NE-response (% baseline I_{Ca})*	*I_{Ca} density (pA/pF)*
GPR18 D118T	1.3 ± 0.04 (13)	36.7 ± 3.1 (13)	-28.5 ± 3.5 (13)
ADRA2A D130T	2.2 ± 0.23 (18) #	42.9 ± 5.0 (16)	-22.8 ± 3.1 (18)
GPR18 D118A	1.2 ± 0.03 (23)	46.2 ± 3.2 (22)	-23.6 ± 2.6 (23)
ADRA2A D130A	1.8 ± 0.19 (12) #	35.3 ± 4.5 (12)	-25.1 ± 3.4 (12)
GPR18 N40A	1.3 ± 0.04 (14)	43.6 ± 2.3 (13)	-29.4 ± 3.3 (14)
ADRA2A N51A	2.6 ± 0.21 (11) #	74.8 ± 11.1 (6) #	-23.9 ± 4.8 (11)
GPR18 I231E	1.2 ± 0.04 (5)	40.8 ± 6.8 (5)	-17.7 ± 3.8 (5)
ADRA2A T373E	2.1 ± 0.3 (7) #	32.7 ± 3.5 (6)	-22.1 ± 3.3 (7)
Uninjected	1.3 ± 0.03 (14)	39.9 ± 2.8 (13)	-34.1 ± 4.1 (14)
ADRA2A	1.6 ± 0.2 (14)	35.6 ± 5.5 (14)	-20.8 ± 2.8 (13)

Molecular Pharmacology Fast Forward. Published on October 25, 2012 as DOI: 10.1124/mol.112.081182
This article has not been copyedited and formatted. The final version may differ from this version.

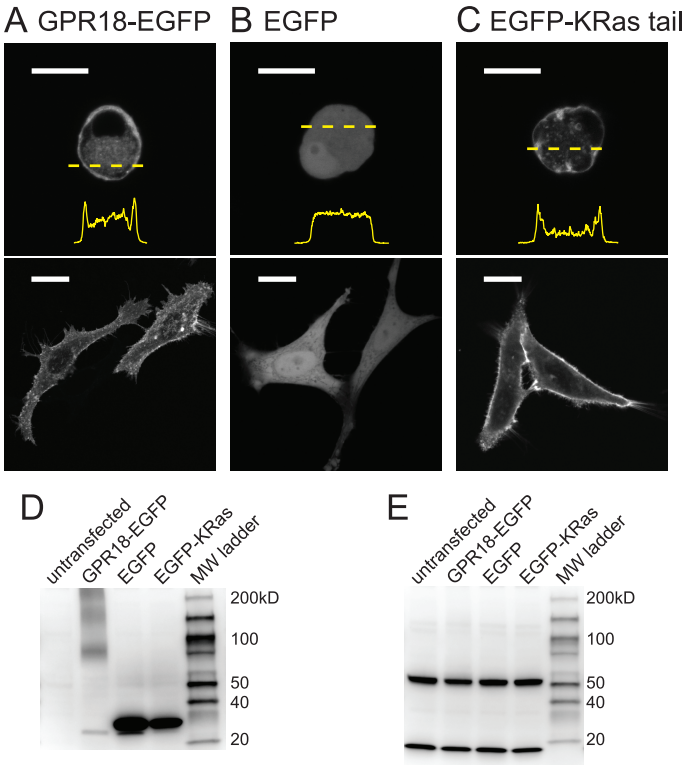

Figure 1

Molecular Pharmacology Fast Forward. Published on October 25, 2012 as DOI: 10.1124/mol.112.081182
This article has not been copyedited and formatted. The final version may differ from this version.

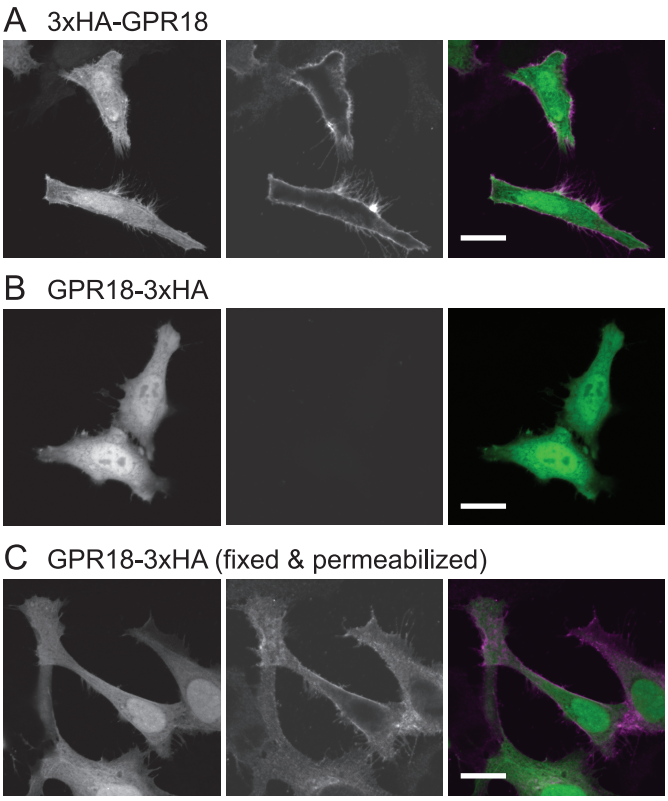

Figure 2

Molecular Pharmacology Fast Forward. Published on October 25, 2012 as DOI: 10.1124/mol.112.081182
This article has not been copyedited and formatted. The final version may differ from this version.

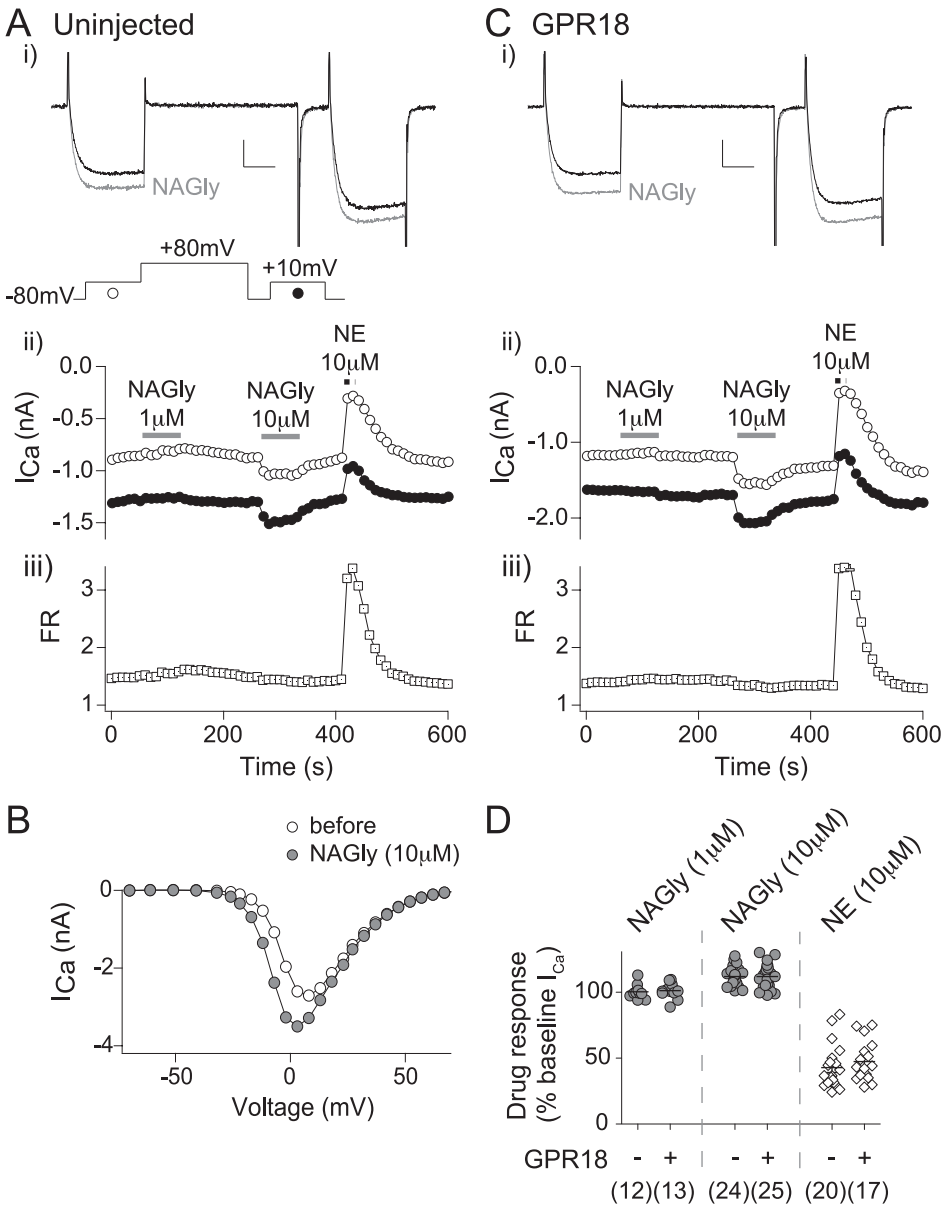

Figure 3

Molecular Pharmacology Fast Forward. Published on October 25, 2012 as DOI: 10.1124/mol.112.081182
This article has not been copyedited and formatted. The final version may differ from this version.

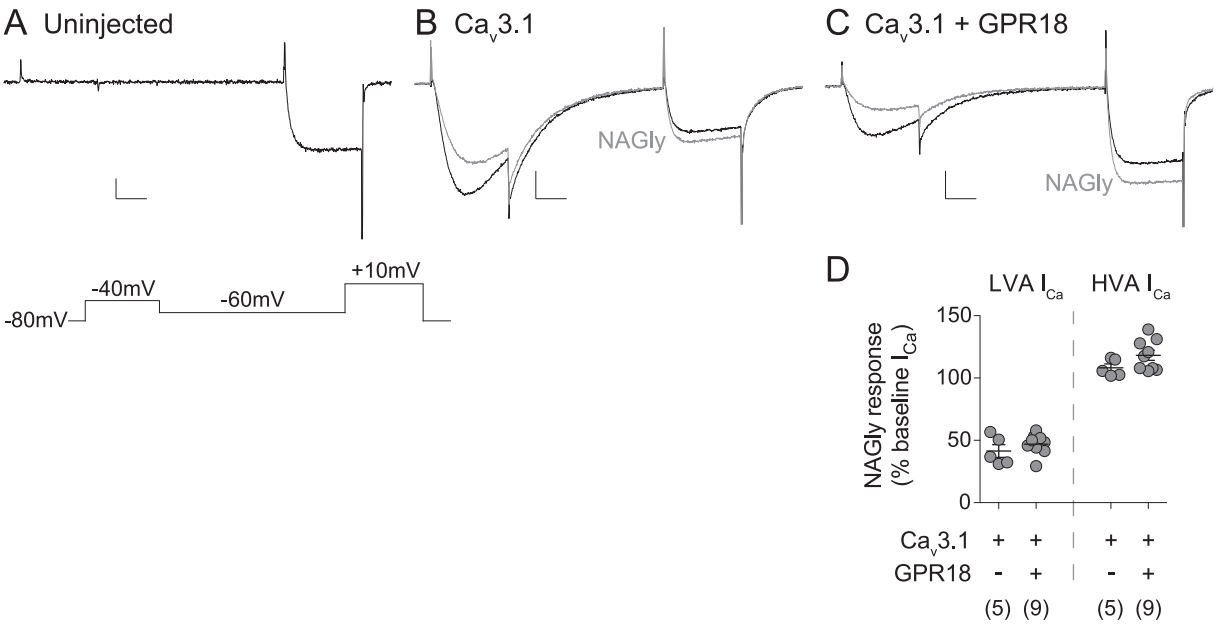

Figure 4

Molecular Pharmacology Fast Forward. Published on October 25, 2012 as DOI: 10.1124/mol.112.081182
This article has not been copyedited and formatted. The final version may differ from this version.

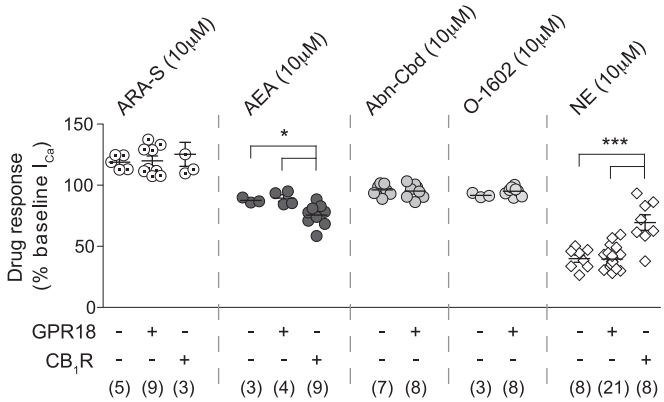

Figure 5

Molecular Pharmacology Fast Forward. Published on October 25, 2012 as DOI: 10.1124/mol.112.081182
This article has not been copyedited and formatted. The final version may differ from this version.

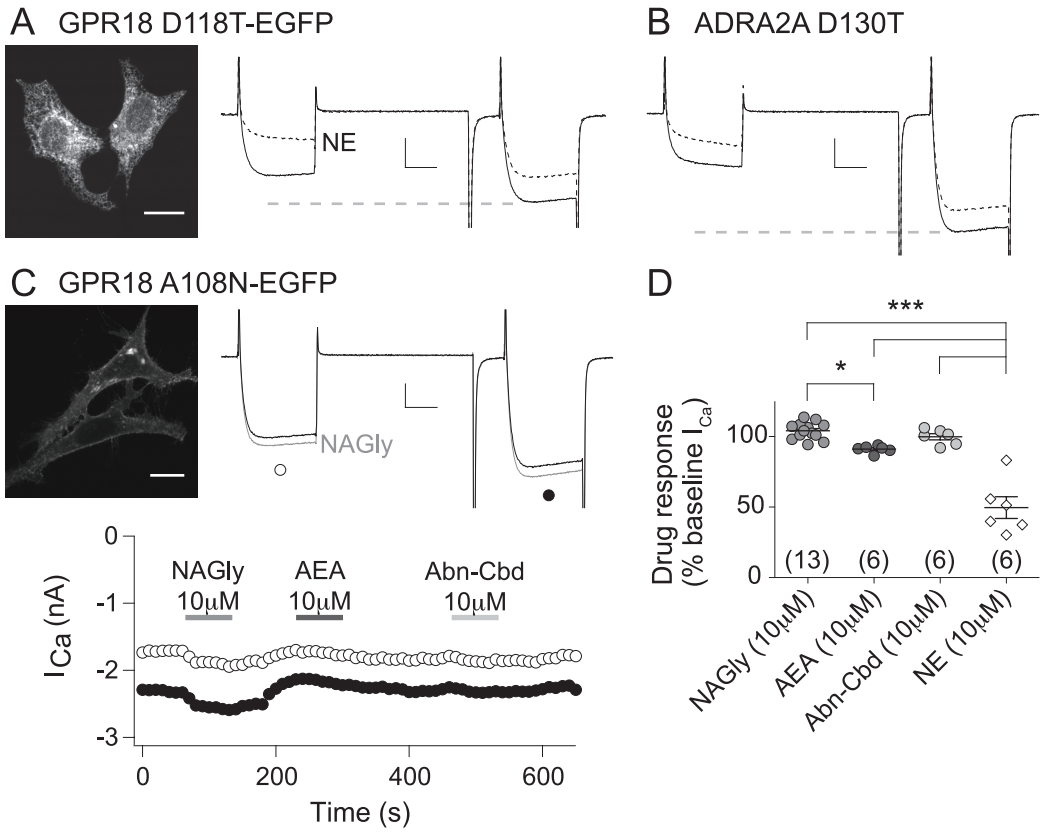

Figure 6

Molecular Pharmacology Fast Forward. Published on October 25, 2012 as DOI: 10.1124/mol.112.081182
This article has not been copyedited and formatted. The final version may differ from this version.

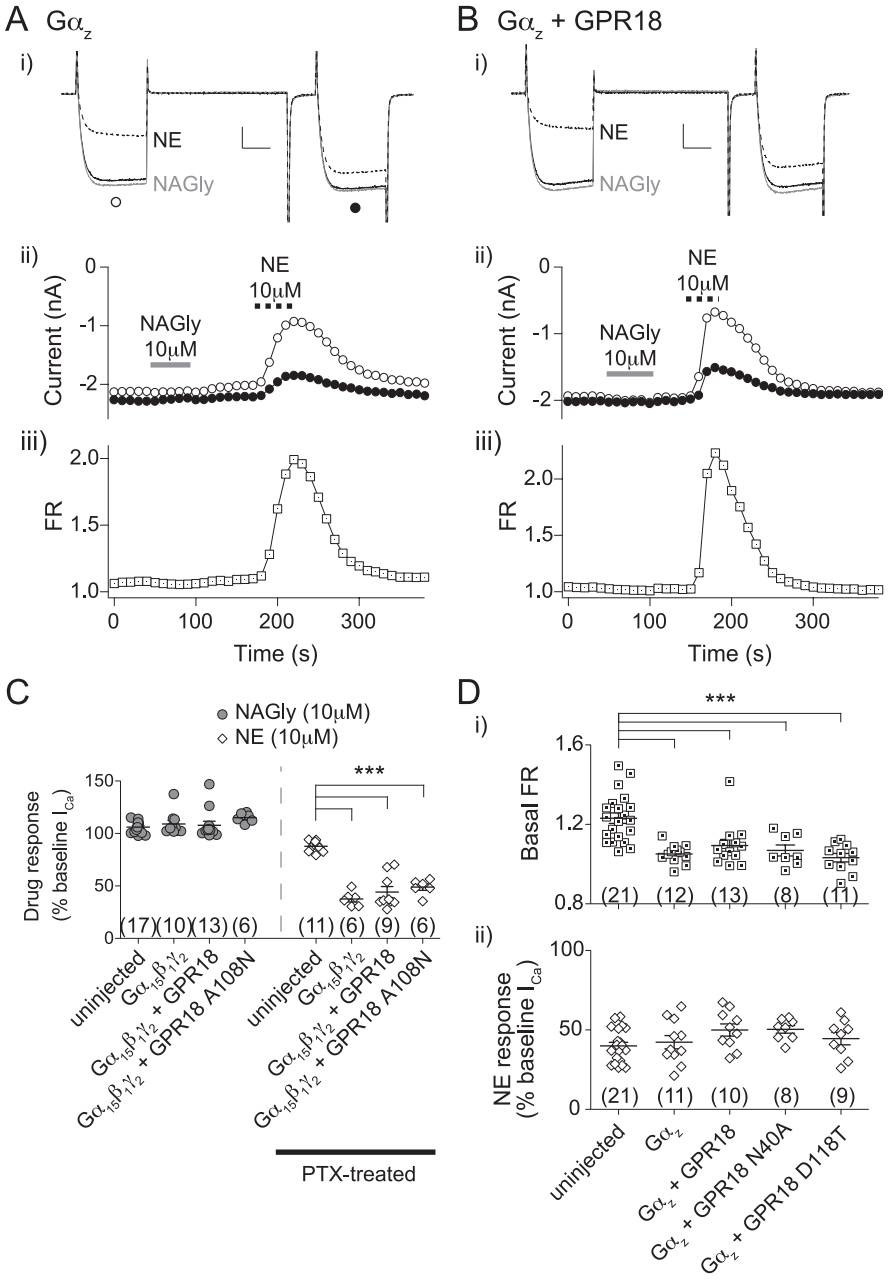

Figure 7

Molecular Pharmacology Fast Forward. Published on October 25, 2012 as DOI: 10.1124/mol.112.081182
This article has not been copyedited and formatted. The final version may differ from this version.

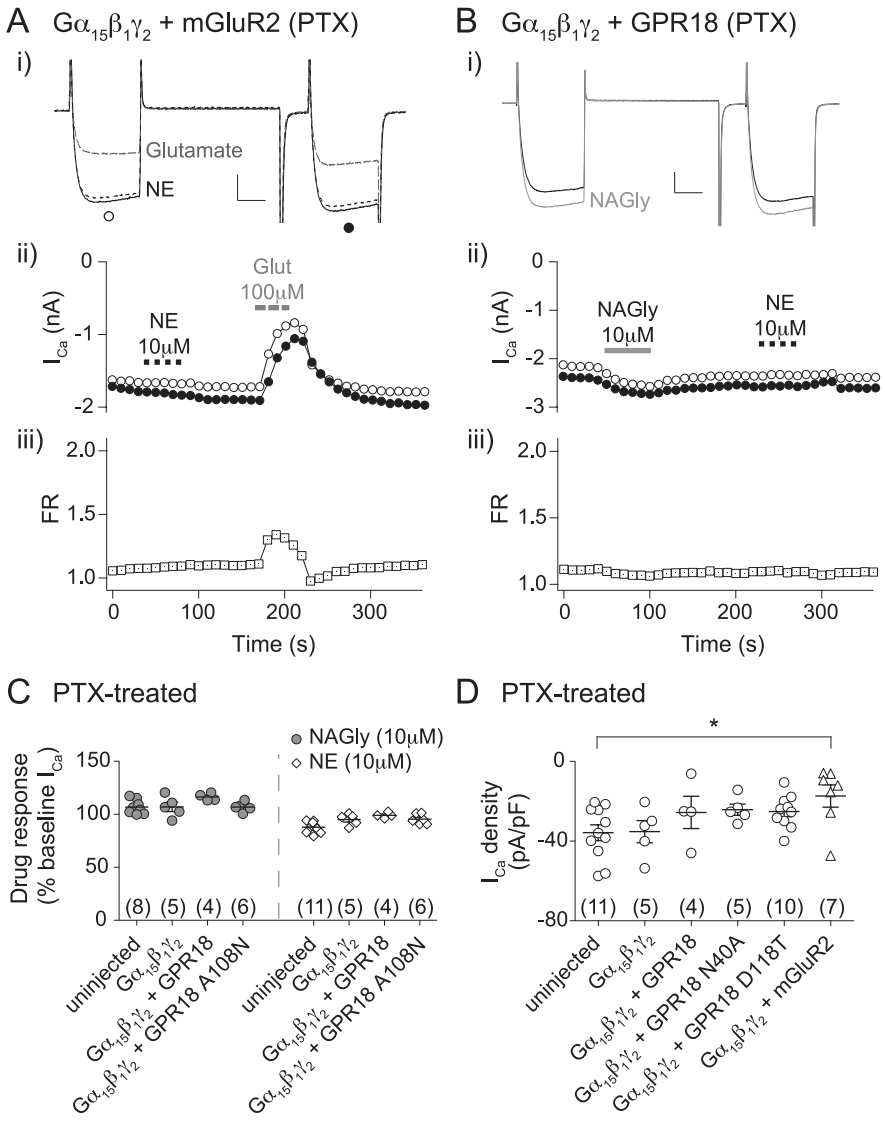

Figure 8

Molecular Pharmacology Fast Forward. Published on October 25, 2012 as DOI: 10.1124/mol.112.081182
This article has not been copyedited and formatted. The final version may differ from this version.

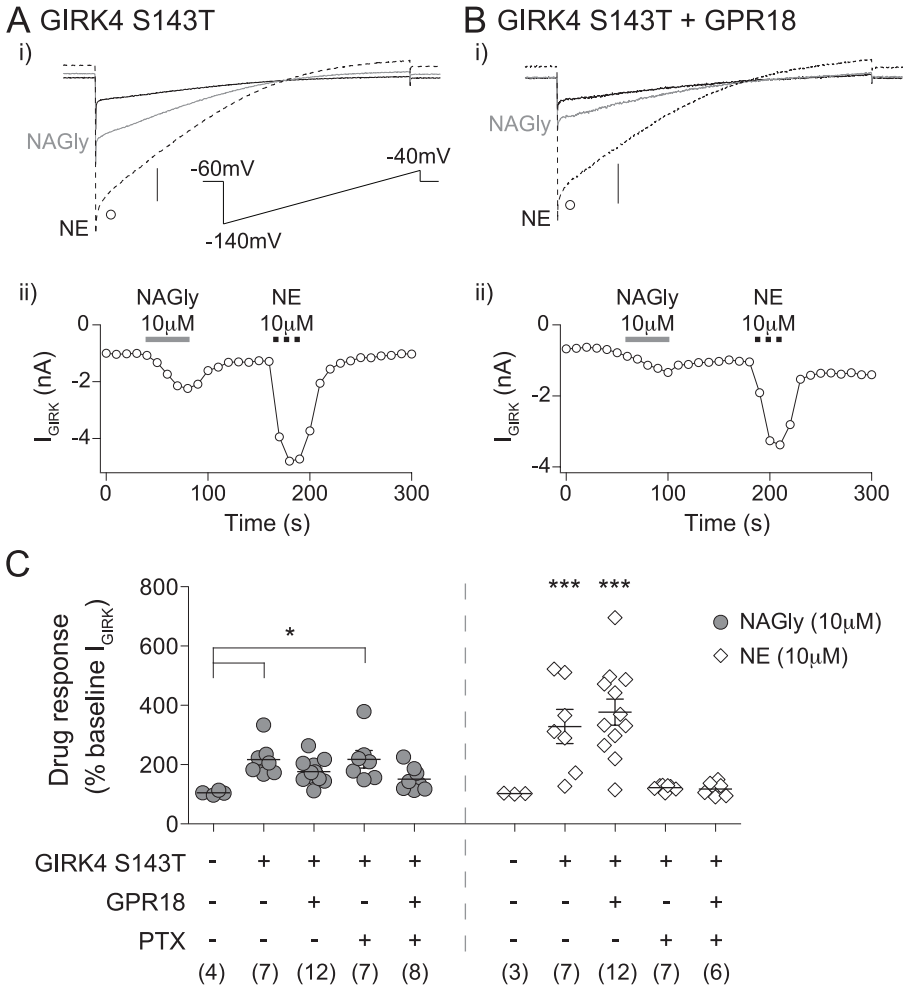

Figure 9

Molecular Pharmacology Fast Forward. Published on October 25, 2012 as DOI: 10.1124/mol.112.081182
This article has not been copyedited and formatted. The final version may differ from this version.

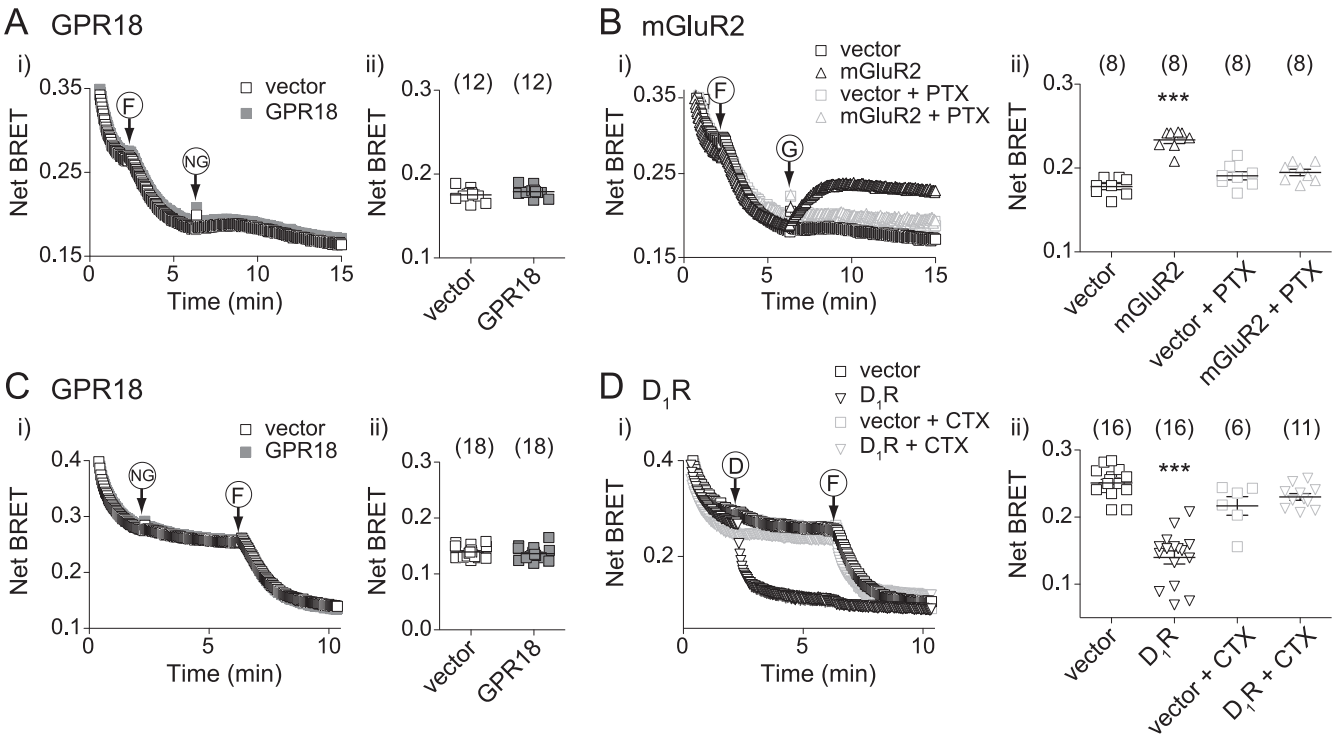

Figure 10